## *PUCK: A Novel Regulator of Arabidopsis Secondary Growth*

STATHAM, KATY,EMMA

# *PUCK:* A Novel Regulator of *Arabidopsis* Secondary Growth

Katy Emma Statham

MSc by Research

Department of Biosciences

Durham University

2025

**Table of Contents**

**List of Abbreviations**

ARF = AUXIN RESPONSE FACTOR

ARR = ARABIDOPSIS RESPONSE REGULATOR

AtHB8 = Arabidopsis Homeobox gene 8

BAK1 = BRI1-ASSOCIATED KINASE 1

BES1 = BRI1- EMS-SUPPRESSOR1

BIL1 = BIN2-LIKE 1

BIN2 = BRASSINOSTEROID-INSENSITIVE 2

CAIL = CAMBIUM-EXPRESSED AINTEGUMENTA-LIKE

CLE41/44 = CLAVATA3-LIKE/EMBRYO SURROUNDING REGION 41/44

CLV1/3 = CLAVATA 1/3

EPFs = EPIDERMAL PATTERNING FACTORS

EPFL = EPF-LIKE

ER = ERECTA

ERf = ER family

ERF = ETHYLENE RESPONSE FACTOR

ERL1 = ERECTA-LIKE 1

GA = gibberellins

GSK3 = Glycogen Synthase Kinase 3

IRX3 = IRREGULAR XYLEM 3

LBD4 = LATERAL ORGAN BOUNDARIES DOMAIN 4

LIN = LUMPY INFECTIONS

LR = lateral root

LRR = leucine-rich repeat

MP = MONOPTEROS

PIF = Phytochrome-interacting factor

PUCK = named after the malevolent pixie from Shakespear's A Midsummer Night's Dream

PXf = PXY family

PXL1/2 = PXY-LIKE 1/2

PXY = PHLOEM INTERCALATED WITH XYLEM (TDR)

RAM = root apical meristem

RLK = receptor-like kinase

SAM = shoot apical meristem

SERK = SOMATIC EMBRYOGENESIS RECEPTOR KINASE

SHR = SHORTROOT

SIEL = SHR INTERACTING EMBRYONIC LETHAL

SUC2 = SUCROSE TRANSPORTER 2

TDIF = TRACHEARY ELEMENT DIFFERENTIATION INHIBITORY FACTOR

TDR = TDIF RECEPTOR (PXY)

TMO6 = TARGET OF MONOPTEROS 6

VC = vascular cambium

VND6 = VASCULAR-RELATED NAC DOMAIN 6

VPY = VAPYRIN

WOX4/14 = WUSCHEL-RELATED HOMEOBOX 4/14

WUS = WUSCHEL

XVP = XYLEM DIFFERENTIATION DISRUPTION OF VASCULAR PATTERNING

**Acknowledgements**

I would like to thank my supervisor, Dr Peter Etchells, for his support and guidance throughout my Masters studies and the opportunities he has given me. Thank you also to Dr Agnieszka Gladala-Kostarz for taking the time to teach me so much in the lab. It has been a pleasure to work with all the members of lab 1004, I appreciate the help everyone has given me with my experiments. The Biosciences Bioimaging facility has provided technical support for microscopy and imaging. The work in this thesis builds upon the PhD project of Dr Wafa Aladadi.

**Abstract**

*PUCK*: A Novel Regulator of *Arabidopsis* Secondary Growth

Katy Emma Statham

Secondary growth is thickening of the plant stem, hypocotyl and root, providing structural support and increased nutrient transport to the growing plant. The main driver of secondary growth is the vascular cambium, a bifacial stem cell population which gives rise to xylem and phloem via organised cell division and differentiation. The TRACHEARY ELEMENT DIFFERENTIATION INHIBITORY FACTOR (TDIF) peptide ligand diffuses into the cambium and signals to the PHLOEM INTERCALATED WITH XYLEM (PXY) receptor-like kinase to promote cell division, vascular organisation and repress xylem identity. However, several aspects of TDIF and PXY biosynthesis, turnover and signalling are not fully understood, in part because all the factors involved have not yet been identified. CLE41 (CLAVATA3/EMBRYO SURROUNDING REGION 41) is the precursor of TDIF. *35S::CLE41* lines, characterised by ectopic cambium, were used in a mutagenesis screen to identify novel TDIF-PXY signalling components. This screen identified *PUCK,* which contains WD40 repeat domains functioning in protein-protein interactions, as a suppressor of *35S::CLE41.* Here, GUS transcriptional reporter analysis revealed that *PUCK* is expressed in the phloem and xylem parenchyma. Histochemical staining identified how *puck* affects the differentiated vascular tissue. *pxy puck* mutants showed a significantly increased xylem width, but no increase in xylem vessels, suggesting *PUCK* does not regulate xylem differentiation. *pxy puck* mutants showed a significantly decreased phloem width compared to wild type, but a significantly wider phloem than *pxy* single mutants. This suggests that *PUCK* may repress phloem differentiation within the TDIF-PXY pathway. It is hypothesised that PUCK may be a scaffold protein involved in influencing phloem production. Lignified xylem vessels make up woody tissue, therefore, understanding secondary growth could allow manipulation of wood formation to increase forest productivity. Secondary growth also provides stability to plant stems and the phloem allows reallocation of resources, manipulation of which could be useful for increasing climate resilience.

## 1.0 Introduction

### 1.1 Background and importance

In order to respond to the ever-changing environment despite their immobility, plants maintain pluripotent stem cell populations to allow post-embryonic growth (Etchells et al., 2016). Typically, when a stem cell divides, one daughter retains stem cell fate to maintain the population while the other differentiates, allowing growth (Serra et al., 2022). These stem cells are found in niches called meristems in the shoot, root and vascular tissue (Etchells et al., 2016). Coordination of these niches is required across space and time to enable organisation and growth control to meet plant needs. There is a high level of conservation between the molecular mechanisms that regulate meristems, however, many components in this maintenance are yet to be understood (Gaillochet and Lohmann, 2015). The shoot and root apical meristems (SAM/RAM) are the most well-characterised, whereas, the meristem in the stem of the plant, the vascular cambium, and its role in radial growth is less well understood (Gaillochet and Lohmann, 2015; Schoof et al., 2000).

Vascular tissue consists of xylem which transports water, and phloem which transports photosynthate around the plant (Figure 1A). The vascular cambium is a bifacial stem cell population controlling cell division, organisation and differentiation of vascular tissues, to allow secondary growth (Etchells et al., 2016). Secondary growth is the thickening of the plant stem and hypocotyl via periclinal cell proliferation and differentiation, providing structural support and increasing nutrient transport to the actively growing plant material (Figure 1B) (Etchells et al., 2016; Turley and Etchells, 2022). Secondary growth occurs in two phases; in phase one the xylem and phloem tissues are produced at the same rate and only xylem vessel elements mature. This means the xylem consists of xylem parenchyma and xylem vessel elements at this stage (Chaffey et al., 2002). This is followed by phase two with accelerated xylem expansion and xylem fibre differentiation also occurring (Chaffey et al., 2002; Ragni and Hardtke, 2014; Ragni et al., 2011; Sibout et al., 2008). Flowering triggers the shift between phases one and two, initiating the expansion of the xylem tissue by the production of mobile shoot-derived gibberellins (GA) (Ragni et al., 2011; Sibout et al., 2008).

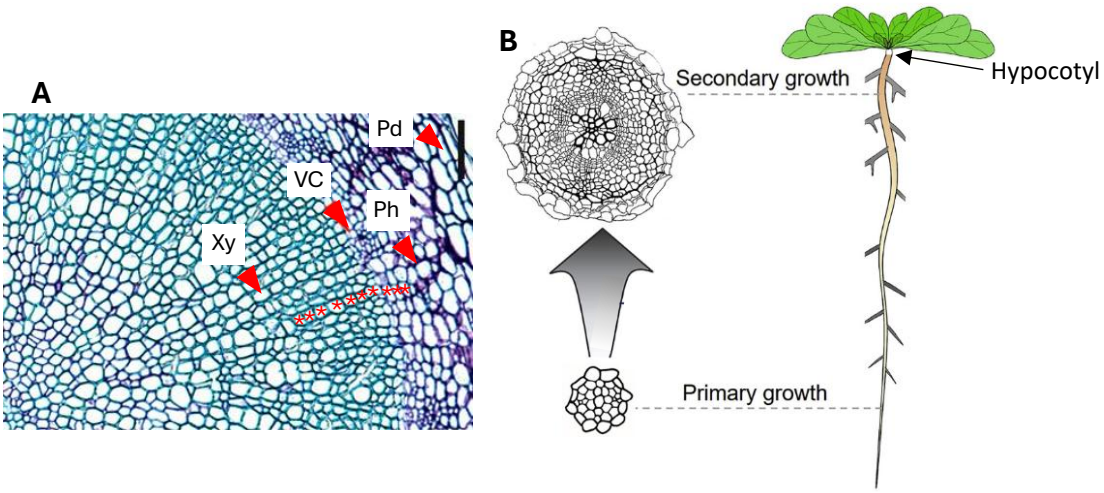


Figure 1, The structure of the vascular tissue and secondary growth in the *Arabidopsis* hypocotyl. A, The structure of the xylem (Xy), vascular cambium (VC), phloem (Ph), and periderm (Pd) tissues in the *Arabidopsis* hypocotyl (Wang et al., 2019). Red stars show a cell file. B, Diagrammatic representation of secondary growth via radial expansion of the hypocotyl (Ye et al., 2021).

Woody tissue in the stem, made up of xylem with lignified secondary cell walls, forms the majority of plant biomass (Etchells et al., 2016). Understanding the mechanism of secondary growth could allow manipulation of wood formation, which could be applied to increasing forest productivity and renewable biofuel generation (Etchells et al., 2016). Secondary growth also functions as a carbon sink and generates carbohydrates in root and tuber crops (Turley and Etchells, 2022). Since the phloem is responsible for nutrient transport, controlling secondary growth could be key to ensuring resources are allocated to where they are needed for plant growth under climate stress (Etchells et al., 2016). In addition to this, the phloem also transports RNAs, phytohormone and electrical signals in stress responses (Hilleary and Gilroy, 2018; Turley and Etchells, 2022). Being able to control phloem production could allow optimisation of signal transduction around the plant, allowing efficient response to novel stressors. In woody and some herbaceous plants, an additional lateral meristem exists in the periderm of the stem and hypocotyl: the cork cambium, or phellogen (Serra et al., 2022). This controls bark production and allows coordinated secondary growth between tissues (Serra et al., 2022).

*Arabidopsis thaliana* (*Arabidopsis*) can be used as a model organism for studying secondary growth since it undergoes root and stem secondary thickening and has conserved genetic regulators across some crop and tree species, including Poplar (*Populus spp.*) (Turley and Etchells, 2022). Secondary growth is most clear in the

hypocotyl since there is no parallel elongation as seen in the stem (Ragni and Hardtke, 2014). Phase two of hypocotyl secondary growth in particular resembles wood production in tree species, making the hypocotyl a good model for investigating secondary growth in trees (Chaffey et al., 2002; Ragni and Hardtke, 2014; Ragni et al., 2011). Understanding secondary growth in the *Arabidopsis* model could therefore provide insight into the processes controlling wood production in trees such as Poplar, which could aid increased productivity in forestry (Chaffey et al., 2002).

## 1.2 Identification of the TDIF-PXY pair in secondary growth regulation

The presence of a peptide ligand and leucine-rich repeat receptor-like kinase (LRR-RLK) pair involved in stem cell maintenance is conserved across meristems (Gaillochet and Lohmann, 2015). This pair acts to mediate gene expression changes via a downstream signalling pathway. In the SAM, the CLAVATA3 (CLV3) ligand is sequestered by the CLV1 receptor, affecting downstream transcription factors (TFs) (Etchells et al., 2016). These TFs include WUSCHEL (WUS) which specifies stem cell maintenance, among others (Mayer et al., 1998). CLV3, CLV1 and WUS form a negative feedback loop, maintaining meristem size (Figure 2) (Lenhard and Laux, 2003; Schoof et al., 2000). WUS induces expression of CLV3, which in turn restricts WUS signalling to a specific organiser domain within the meristem while also specifying organ initiation outside of the stem cell niche (Lenhard and Laux, 2003; Schoof et al., 2000). This CLV3-WUS feedback loop controls growth of aboveground plant organs including new leaves or inflorescences. In the RAM, a similar maintenance system exists, supplying cells for underground tissue growth (Gaillochet and Lohmann, 2015).

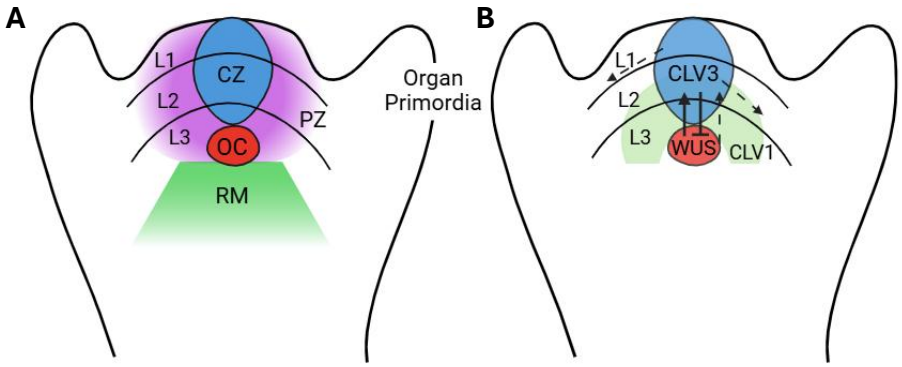


Figure 2, The structure of the shoot apical meristem (SAM) and the signalling factors controlling its maintenance. A, Organisation of the SAM subdomains showing the central zone (CZ), organising centre

(OC), rib meristem (RM), peripheral zone (PZ) and stem cell layers (L1-3), adapted from (Miyashima et al., 2012; Uchida and Torii, 2019). B, CLV1, CLV3 and WUS expression domains, solid arrows show expression changes, dotted arrows show protein movement, adapted from (Lenhard and Laux, 2003; Yadav et al., 2013).

In the vascular cambium, the TRACHEARY ELEMENT DIFFERENTIATION INHIBITORY FACTOR (TDIF) ligand is detected by the PHLOEM INTERCALATED WITH XYLEM (PXY) receptor, affecting TFs such as WUSCHEL-RELATED HOMEOBOX 4/14 (WOX4/14) (Figure 3) (Etchells et al., 2016). This system regulates cambium initiation, cell proliferation, vascular organisation and repression of xylem differentiation within the cambial zone (Etchells et al., 2016). TDIF-PXY function is conserved across *Arabidopsis* and Poplar species with multiple orthologous genes identified (Turley and Etchells, 2022). TDIF-PXY signalling is also involved in lateral root (LR) development; *PXY* is expressed during LR initiation and mutants show altered LR density (Cho et al., 2014). This shows that the ligand-receptor system is widespread with multiple different functions throughout the plant.

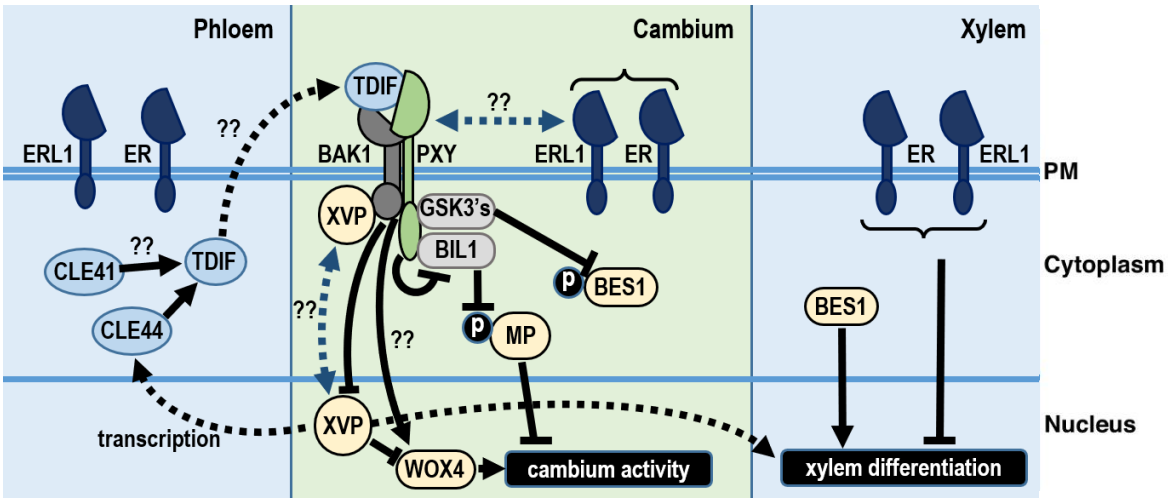


Figure 3, A diagram showing the localisation and putative downstream components of TDIF-PXY signalling in the phloem, cambium and xylem. The nucleus, cytoplasm and plasma membrane (PM) are labelled. Blue bubbles show PXY ligand components, yellow bubbles show transcription factors, grey bubbles show GSK3s, RLKs are within the PM. Arrows indicate positive interaction, blunt arrowheads indicate inhibition, dotted arrows indicate translocation. Question marks show where knowledge is missing within the network. (This includes how CLE41 produces TDIF, how TDIF translocates to the cambium, what triggers XVP to translocate to the nucleus, and limited evidence for a PXY-ER interaction). P indicates phosphorylation. TDIF is produced in the phloem and then translocates to the vascular cambium, where it binds to PXY and its co-receptors. This produces a signalling cascade which controls multiple downstream responses including cambium initiation, cell proliferation, vascular organisation

and repression of xylem differentiation within the cambial zone. Adapted from (Bagdassarian et al., 2020).

TDIF was identified as an extracellular factor inhibiting tracheary element differentiation in a transdifferentiation assay where mesophyll cells were transdifferentiated to xylem (Ito et al., 2006). Mass spectrometry and amino acid sequencing revealed that it is a dodecapeptide (Ito et al., 2006). Homology searches showed that TDIF is derived from the *CLAVATA3/EMBRYO SURROUNDING REGION (CLE)* genes *CLE41, CLE42* and *CLE44* (Etchells and Turner, 2010a; Ito et al., 2006)(Figure 3). However, it is unknown how these proteins are cleaved to form the mature peptide (Etchells et al., 2016). Addition of TDIF inhibited xylem differentiation and promoted cell division in cultured cells and *in planta* (Hirakawa et al., 2008; Ito et al., 2006). *CLE* overexpression lines support this hypothesis that TDIF functions to promote cell division (Etchells et al., 2016). Disorganised vascular tissue was seen in plants engineered for constitutive or xylem-specific TDIF overexpression, but not phloem-specific overexpression, suggesting ligand localisation and not expression level is important for function (Etchells and Turner, 2010a).

To identify the TDIF receptor, RLK mutants were treated with TDIF and those that failed to respond were considered to contain mutations in potential receptors (Hirakawa et al., 2008). Photoaffinity labelling was used to confirm the identification of TDIF RECEPTOR (TDR/PXY), encoded by the gene *PXY* (Etchells et al., 2016; Hirakawa et al., 2008). *PXY* is closely related to *CLV1,* showing conservation between the SAM and the vascular cambium (Hirakawa et al., 2008). PXY is an LRR-RLK with plasma membrane subcellular localisation; it contains an extracellular LRR ligand binding domain, a transmembrane domain, and a cytoplasmic kinase domain for coordinating downstream signalling upon TDIF perception (Fisher and Turner, 2007; Hirakawa et al., 2008; Turley and Etchells, 2022). β-glucuronidase (GUS) reporter gene fusions and *in situ* hybridisation demonstrated that *PXY* is expressed in the cambium, while *CLE41* and *CLE44* are expressed in the phloem (Figure 3) (Etchells and Turner, 2010a; Hirakawa et al., 2008). Antibody labelling of TDIF showed that it is secreted from the phloem cells (Hirakawa et al., 2008). The differing expression localisations and mobility of TDIF suggests that it conveys positional information to PXY (Etchells and Turner, 2010a). *pxy* mutants demonstrated a lack of vascular organisation and ectopic xylem

differentiation, consistent with TDIF results (Etchells and Turner, 2010b). Importantly, *CLE41/42* overexpression phenotypes are repressed by *pxy*, therefore, it is thought that all TDIF signalling occurs via the PXY receptor (Etchells and Turner, 2010a).

The mutant screen which identified *PXY* in *Arabidopsis*, also identified two homologues, PXY-LIKE 1 (PXL1) and PXL2 which are also RLKs (Fisher and Turner, 2007). It is common in *Arabidopsis* to have genes in multiple copies and this needs to be accounted for when generating mutants and characterising gene functions. While *pxl1/2* mutants alone did not show an obvious phenotype, *pxy pxl1* and *pxy pxl2* double mutants enhanced the *pxy* mutant vascular phenotype. This shows that *pxy* and *pxl1/2* interact to regulate vascular development (Fisher and Turner, 2007). However, organisation is not completely disrupted in these mutants suggesting there may be other regulating factors with compensatory function (Fisher and Turner, 2007).

A vascular cambium organiser has been identified, demonstrating conservation with the SAM. Smetana et al. (2019) used lineage tracing to identify that vascular cambium stem cells form adjacent to cells of xylem identity in the root vascular tissue. It is hypothesised that this specification of stem cell identity in neighbouring cells must occur prior to the programmed cell death in differentiated xylem vessels (Smetana et al., 2019). During growth, the organiser cells can differentiate to mature xylem vessels and new cells from the vascular cambium then acquire organiser identity, allowing radial expansion (Smetana et al., 2019). The stem cell organiser is defined by a local auxin maximum; auxin signalling via ARF TFs, including MONOPTEROS (MP), was found to promote HD-ZIP III genes (Smetana et al., 2019). Several studies have shown that HD-ZIP III TFs positively regulate xylem identity (Baima et al., 2001; Carlsbecker et al., 2010; Emery et al., 2003; Ohashi-Ito et al., 2005). miRNAs suppress HD-ZIP III TF function, to control xylem patterning (Carlsbecker et al., 2010; Emery et al., 2003; Ohashi-Ito et al., 2005; Zhou et al., 2007). Inducible miRNA downregulation and mutation of the HD-ZIP III TF AtHB8 showed that this TF not only regulates xylem cell fate but can also specify xylem cells as stem cell organisers (Baima et al., 2001; Smetana et al., 2019). Transcriptomics, mutant analysis and computational modelling identified that the stem cell organisers, regulated by auxin, non-cell autonomously confer stem cell identity to neighbouring cells by inducing CAIL (CAMBIUM-EXPRESSED AINTEGUMENTA-LIKE) TFs downstream of PXY, generating the vascular cambium

(Eswaran et al., 2024). However, the mechanism via which TDIF-PXY promotes CAIL TFs is not yet clear.

Since photosynthesis requires both light and water, these resources need to be coordinated for plant growth (Ghosh et al., 2022). Consistent with this idea, vascular development has been found to be triggered by light, ensuring xylem differentiation occurs at a rate which allows sufficient water and minerals to be transported to the photosynthesising tissues to meet growth demand (Ghosh et al., 2022). Ghosh et al. (2022) found using time-course transcriptional analysis, monochromatic light treatment and overexpression and loss-of-function lines that, in the dark, PIF TFs accumulate and induce *CLE44* expression. *CLE44* induction leads to TDIF production and subsequent repression of xylem differentiation and maintenance of the stem cell niche. In the light, PIFs are inactivated by photoreceptors meaning *CLE44* expression is decreased, reducing TDIF production allowing more xylem differentiation to occur (Ghosh et al., 2022).

In addition to the PXY family (PXf), other RLKs have been found to function in secondary growth regulation and interact with PXY. Structural and genetic studies suggest that the plasma membrane SOMATIC EMBRYOGENESIS RECEPTOR KINASE (SERK) co-receptor, BRI1-ASSOCIATED KINASE 1 (BAK1), is needed for activation of PXY signalling upon TDIF perception (Figure 3) (Zhang et al., 2016). Fisher & Turner (2007) found that in the Landsberg erecta (Ler) ecotype, the *pxy* phenotype was more severe. As Ler carries an *ERECTA* (*ER*) mutation, it was suggested that ER, also an RLK, may be involved in vascular development, among its wide-ranging functions across the plant (Fisher and Turner, 2007; Torii et al., 1996) (see section 1.4).

### 1.3 Downstream factors in TDIF-PXY signalling

To identify the downstream TFs activated by TDIF-PXY, gene expression changes were measured upon incubation with TDIF in wild-type (WT) and *pxy* mutants (Etchells et al., 2013; Hirakawa et al., 2010). *WOX4* and *WOX14* expressions were found to be activated by TDIF in WT but not *pxy* (Etchells et al., 2013; Hirakawa et al., 2010). Reduced proliferation in *wox4* mutants suggests that this gene promotes cell division, however, xylem differentiation was not suppressed (Hirakawa et al., 2010). Analysis of

*wox4 wox14* double mutants demonstrate that these genes act redundantly, downstream of PXY, but do not affect vascular organisation (Etchells et al., 2013). Multiple genetically separable downstream pathways must, therefore, exist for the TDIF-PXY pair to independently control cell division, organisation and xylem differentiation of the vascular tissue (Etchells et al., 2016).

To identify more downstream signalling components, broad LRR-RLK signalling was investigated, and it was found that Glycogen Synthase Kinase 3 (GSK3) proteins are involved (Figure 3) (Etchells et al., 2016). Yeast two-hybrid assays and fluorescence resonance energy transfer (FRET) identified that the GSK3 BRASSINOSTEROID-INSENSITIVE 2 (BIN2) interacts with PXY at the plasma membrane (Cho et al., 2014; Kondo et al., 2014). gsk3 mutants showed increased xylem differentiation upon TDIF treatment, with no effect on cambial cell division; GSK3s repress xylem differentiation in the TDIF-PXY pathway to maintain the meristem (Kondo et al., 2014). The pathways involving GSK3s and WOX4/14 act in parallel, downstream of PXY, to control xylem differentiation and cell division, respectively (Turley and Etchells, 2022). Cho et al. (2014) used *bin2* mutants to show that TDIF-PXY signalling can affect LR density via the BIN2-AUXIN RESPONSE FACTOR (BIN2-ARF) pathway. BIN2 phosphorylates ARF7/19, releasing them from their repressor (Cho et al., 2014). This demonstrates the varied outputs of this signalling mechanism in different localisations.

Smit et al. (2020) generated a transcriptional regulatory network using enhanced yeast one-hybrid assays to identify TFs interacting with promoters of PXY signalling. Using this model and *35S::CLE41* expression analysis*,* WOX14, TMO6 (TARGET OF MONOPTEROS 6) and LBD4 (LATERAL ORGAN BOUNDARIES DOMAIN 4) were predicted to form a feedforward loop (Smit et al., 2020). *In situ* hybridisation and GUS expression confirmed that these genes are expressed simultaneously in the same localisation of the inflorescence stem vasculature. *tmo6 wox14* and *tmo6 wox14 lbd4* lines were identical, confirming that LBD4 is downstream. Addition of TDIF induced *LBD4* and *TMO6* expression only with functional *WOX4,* demonstrating that *WOX4* is upstream. *lbd3 lbd4* double mutants, accounting for functional redundancy, and *IRX3*:*LBD4* and *SUC2*:*LBD4* constructs, which altered expression domains to the xylem and phloem respectively, showed *LBD4* controls phloem distribution and proliferation (Smit et al., 2020). The *IRX3:CLE41* disorganised phenotype was suppressed by *lbd4,* supporting the

*in situ* hybridisation evidence that *LBD4* contributes to vascular organisation and is expressed at the phloem-cambium boundary (Smit et al., 2020).

A mutant screen identified XYLEM DIFFERENTIATION DISRUPTION OF VASCULAR PATTERNING (XVP), whose mutant showed premature xylem differentiation, reduced proliferation and vascular disorganisation, suggesting TDIF-PXY signalling is affected (Yang et al., 2020a). The structure and transactivation activity confirmed XVP is a NAC TF (Yang et al., 2020a). A mating-based split ubiquitin yeast-two-hybrid system, FRET and GFP-tagging demonstrated that XVP interacts directly with the PXY co-receptor, BAK1, at the plasma membrane in the cambium (Figure 3) (Yang et al., 2020a). *xvp nac048* double mutants, accounting for functional redundancy, showed higher *WOX4* expression and increased proliferation upon addition of TDIF compared to WT, suggesting that XVP negatively regulates PXY signalling (Yang et al., 2020a). Transcriptome analysis showed that XVP acts via the master regulator VASCULAR-RELATED NAC DOMAIN 6 (VND6) to promote xylem differentiation (Yang et al., 2020a). Gene expression analysis showed that while XVP promotes *CLE44* expression, TDIF represses *XVP* in a feedback loop; this is a potential control mechanism for meristem maintenance similar to that seen in the SAM (Yang et al., 2020a). The mechanism of interaction of XVP with WOX4/14, GSK3s or LBD4 is not known.

### 1.4 Other RLKs in secondary growth regulation: ERECTA

As in the PXf, the ER family (ERf) has three homologues. ERECTA (ER), ERECTA-LIKE 1 (ERL1), and ERL2 are RLKs which form ligand-receptor complexes with EPIDERMAL PATTERNING FACTORS (EPFs) or EPF-LIKE (EPFL) peptides (Lee et al., 2012; Shpak et al., 2004; Takata et al., 2013). ER has pleiotropic function, influencing a wide range of developmental processes, including regulating stomatal distribution or inflorescence architecture (Shpak et al., 2003; Shpak et al., 2005; Tisné et al., 2011). In the vascular tissue, ERf RLKs function in an organ-specific manner, promoting growth and organisation in the inflorescence stem while suppressing xylem proliferation and premature fibre differentiation in the hypocotyl (Ikematsu et al., 2017; Turley and Etchells, 2022; Uchida and Tasaka, 2013; Uchida et al., 2012; Wang et al., 2019).

Etchells et al. (2013) proposed an interaction between PXY and ER. In the inflorescence stems, *pxy er* showed vascular organisation defects with no effect on proliferation, supporting the evidence for genetic separation of vascular control. However, in the hypocotyl, *pxy er* showed increased organisational defects and reduced diameter compared to single mutants. These results are difficult to interpret since ER/ERL1 repress xylem expansion in the hypocotyl and there is much functional redundancy in the PXY and ER families, but it is possible that PXY-ER interactions promote proliferation at this localisation (Etchells et al., 2013; Ikematsu et al., 2017). Wang et al. (2019) generated sextuple *pxy pxl1 pxl2 er erl1 erl2* mutants to overcome the functional redundancy in these gene families. Mutant inflorescence stems showed organisational defects and reduced vascular bundle size (Wang et al., 2019). Sextuple mutant hypocotyls could not progress to radial growth, showing organ-specific disorganisation and reduced proliferation (Wang et al., 2019). qRT-PCR was used to identify PXf and ERf gene expression changes in *er* and *pxf* mutants, which allowed identification of genetic interactions between these gene families across the stem and hypocotyl (Wang et al., 2019).

Direct ERf-PXf RLK interaction is possible due to overlapping expression patterns seen in hypocotyls and *in vitro* evidence, however further research is needed to confirm this *in vivo* (Turley and Etchells, 2022; Wang et al., 2019) (Figure 3). Downstream signalling components and targets of the ER pathway need to be elucidated to understand the molecular basis of PXY-ER interaction and the level of conservation between these pathways (Turley and Etchells, 2022).

### 1.5 Phytohormones interacting with the TDIF-PXY pathway

Auxin and cytokinin are known to function cooperatively in cell proliferation and differentiation in the meristem (Han et al., 2018; Schaller et al., 2015). WOX4 is a signal integrator which links the TDIF-PXY regulation of secondary growth to phytohormone signalling (Denis et al., 2017; Etchells et al., 2012; Hirakawa et al., 2010; Hu et al., 2022; Suer et al., 2011). The auxin-dependent TF, MONOPTEROS (MP) negatively regulates stem cell identity by repression of *WOX4* (Brackmann et al., 2018). The GSK3, BIN2-LIKE 1 (BIL1), has been shown to integrate PXY signalling with cytokinin signalling. Han et al. (2018) showed that BIL1 phosphorylates MP to negatively regulate cambium activity

and upregulates the negative regulators of cytokinin signalling, ARABIDOPSIS RESPONSE REGULATOR 7 (ARR7) and ARR15. Within the cambium, TDIF-PXY inhibits BIL1, preventing phosphorylation of MP to allow stem cell maintenance (Han et al., 2018) (Figure 3). This also reduces the effect of MP on ARR7/15 expression, allowing cytokinin signalling in the cambium (Han et al., 2018). Other Auxin Response Factors (ARFs) such as ARF3/4 activate cambial activity, showing how auxin contributes to regulation of the vascular stem cell population (Brackmann et al., 2018).

Strigolactones are also known to promote cambium activity via the TDIF-PXY pathway, and interact with auxin signalling (Agusti et al., 2011). Hu et al. (2022) found that BRI1-EMS-SUPPRESSOR1 (BES1) acts downstream of strigolactone signalling and functions to repress WOX4 by binding its promoter, inhibiting cambium proliferation and promoting differentiation. BES1 is repressed by GSK3s in a TDIF-dependent manner to allow cambium maintenance within the cambial zone, while allowing vascular tissue differentiation outside of this (Kondo et al., 2014) (Figure 3).

Ethylene has been shown to promote radial growth, forming a compensatory pathway with PXY in meristem maintenance (Etchells et al., 2012). Mutant analyses show that in the absence of functional *PXY,* expression of ETHYLENE RESPONSE FACTOR (ERF) TFs is de-repressed, allowing ethylene signalling to take over control of meristem cell proliferation (Etchells et al., 2012). Yang et al. (2020b) identified an ethylene overproducing mutant, *1-aminocyclopropane-1-carboxylate synthase 7 (acs7-d),* which showed using mutant analysis that ethylene is required for cambium maintenance via *WOX4.* The results of these phytohormone studies demonstrate how well-integrated the TDIF-PXY signalling pathway is to the environmental conditions of the plant, allowing growth to be tailored to plant needs.

Thus far, several downstream components and interacting partners have been characterised, however, this has revealed that the TDIF-PXY pathway is complex with many more signalling components still to be identified. Integration of downstream signalling pathways is required to fully understand regulation of this system. Furthermore, TDIF and PXY biosynthesis and turnover are still not well understood. Only once all the factors involved have been identified and integrated can a complete signalling network be generated. An increased level of understanding of the TDIF-PXY

pathway could allow manipulation of this pathway via gene editing or selective breeding to increase wood production, stem strength or nutrient allocation.

## 1.6 *PUCK* is a novel component of TDIF-PXY signalling

A forward genetic screen was used to identify novel downstream components of TDIF-PXY signalling to increase understanding of the network (Aladadi, 2023). Mutagenesis was performed on *35S::CLE41* seed, characterised by constitutively active TDIF-PXY signalling. Morphological and histological comparisons were made to identify putative mutants which restored WT phenotype. Mutants with restored WT phenotype were suggested to have mutations in genes functioning downstream of *CLE41* in the TDIF-PXY pathway (Aladadi, 2023). This led to identification of *PUCK.* The *35S::CLE41* phenotype consists of multiple, early, shorter inflorescences with rounder leaves. These plants also have ectopic cambia showing disorganised hypocotyl vasculature with increased proliferation resulting in greater hypocotyl diameter. *35S::CLE41 puck-1* showed single, tall inflorescences with narrow leaves (Figure 4A-B). This putative mutant also showed organised hypocotyl vasculature similar to that of WT, as well as reduced hypocotyl diameter and cell number compared with *35S::CLE41* (Figure 4C) (Aladadi, 2023).

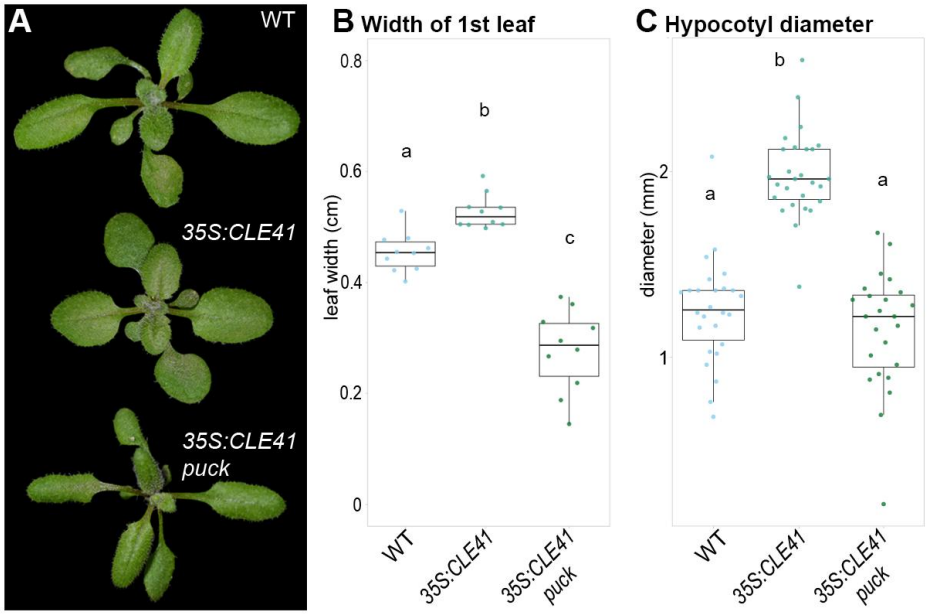


Figure 4, Identification of *PUCK* via mutagenesis screen results. A, Images of WT, *35S::CLE41* and *35S::CLE41 puck-1* rosettes identifying *35S::CLE41 puck-1* restoration to WT phenotype. B, Boxplots showing the width of the first leaf (cm) for WT, *35S::CLE41* and *35S::CLE41 puck-1* genotypes. *35S::CLE41 puck-1* has a narrower leaf width than WT. C, Boxplots showing the hypocotyl diameter (mm) for WT,

*35S::CLE41* and *35S::CLE41 puck-1* genotypes. *35S::CLE41 puck-1* restores WT hypocotyl diameter (Aladadi, 2023).

Once the *PUCK* gene was identified, *puck-2* (SALK_000586) mutants were generated (where *puck-1* refers to the original EMS allele and *puck-2* a T-DNA insertion allele), to confirm that the results seen in *35S::CLE41 puck-1* were in fact due to mutations in the *PUCK* gene (Figure 5A). *IRX3::CLE41 puck-2* mutants were able to restore WT differentiation, organisation and cell division (Figure 5B) (Aladadi, 2023). The *IRX3* xylem-specific promoter was used in addition to the *35S* constitutive promoter, since the change in TDIF localisation to the xylem results in severe organisational and xylem differentiation defects (Etchells and Turner, 2010a). These results show that functional PUCK is required for the *CLE41* overexpression phenotype and, therefore, PUCK likely functions downstream of *CLE41* in the TDIF-PXY pathway. The *puck-2* line was used for further analysis.

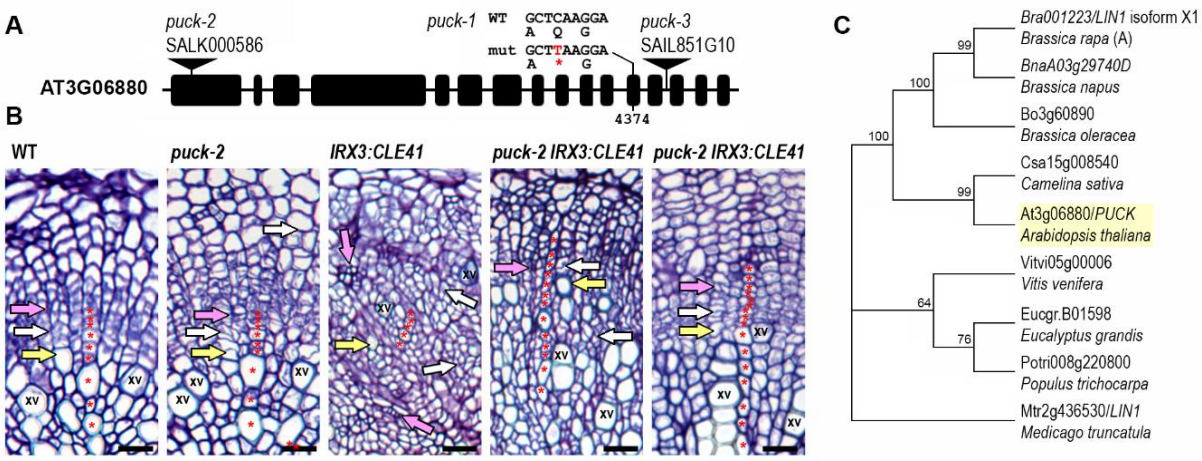


Figure 5, Initial characterisation of *PUCK*. A, *PUCK* gene annotation showing *PUCK* is *Arabidopsis* gene *AT3G06880*. B, Transverse hypocotyl sections of WT, *puck-2, IRX3::CLE41,* and *puck-2 IRX3::CLE41*. Pink arrows mark phloem, white arrows mark cambium, yellow arrows mark xylem. XV marks xylem vessels. Red stars mark cell files. Scale bars 20 µm. C, Dendrogram of *PUCK* and its homologues, including in brassicas and legumes (Aladadi, 2023).

Some differences were detected between *puck-1* and *puck-2* lines. In some cases, *35S::CLE41 puck-2* and *IRX3::CLE41 puck-2* lines showed increased radial growth compared to WT, with no reduction in the number of cells in the vascular tissue compared to *35S::CLE41,* as was seen in *35S::CLE41 puck-1* lines (Aladadi, 2023). Aladadi (2023) also noted that *puck-2* demonstrated increased radial growth compared to WT. It is unclear why these differences are present, however, it is possible that PUCK

functions to balance cell division and proliferation and so could appear to have differing functions depending on the conditions.

Since *puck* suppresses *IRX3::CLE41*, it is hypothesised that *puck* may function in the TDIF-PXY pathway and, therefore, there may be epistasis between *pxy* and *puck*. However, *puck* and *pxy puck* mutants did not show a reduced hypocotyl diameter relative to WT, as was seen in *pxy* alone (JP Etchells, personal communication). In transverse sections, *puck, pxy* and *pxy puck* mutants showed reduced xylem number relative to WT, suggesting *PUCK* may be required for normal xylem formation. While xylem cell type was also analysed, the stain used for these sections made categorising cell types difficult and therefore no conclusions can be confidently drawn from this data. Altogether, these results suggest *puck* may have differing functions throughout the vascular tissue, however, tissue specific staining and investigation into the phloem tissue should be used to confirm these results.

Whole genome sequencing identified the *PUCK* gene as *AT3G06880* (Figure 5A) (Aladadi, 2023). *PUCK* identity was confirmed by mutations in *AT3G06880* suppressing *35S::CLE41*. *PUCK* is a single copy, 5171bp gene with 16 exons, and is a member of the Transducin/WD40 repeat-like superfamily. PUCK contains several WD40 repeat domains and two Armadillo repeats, which are suggested to function in protein-protein interactions and intracellular signalling, respectively (Aladadi, 2023; Coates, 2003; Mishra et al., 2012). This supports the hypothesis from Aladadi (2023) that PUCK is likely downstream in PXY signalling and could be involved in recruiting downstream signalling factors.

To identify *PUCK* homologues, the Multiple Sequence Alignment (MUSCLE) tool provided by the Molecular Evolutionary Genetic Analysis (MEGA11) software was used, supported by data from PANTHER (Aladadi, 2023; Mi et al., 2004). Several homologues were found, including in brassicas, legumes and the *Populus trichocarpa* gene *Potri008G220800* (Figure 5C). One homologue identified in *Medicago truncatula (Medicago), LUMPY INFECTIONS (LIN)* has been studied and its function hypothesised.

In order to form a root nodule, coordination is required between two genetically separable pathways: rhizobial infection and nodule organogenesis (Kiss et al., 2009). In *lin* mutants, nodule development is arrested as a result of aborted rhizobial infection

and, therefore, it was concluded that *LIN* is required for regulating rhizobial colonisation and nodule differentiation from primordia (Kiss et al., 2009; Kuppusamy et al., 2004). Kiss et al. (2009) identified that *LIN* contains a U-box domain with E3 ubiquitin ligase activity, a WD40 repeat domain, and an Armadillo-repeat region, but also contains large regions of unknown function. Mutant analysis showed that the WD40 repeat domain was essential for function (Kiss et al., 2009). It was suggested that the WD40/Armadillo repeat domains may define target specificity or function to regulate post-translational modifications (Kiss et al., 2009). Reporter experiments suggest that *LIN* is present in dividing cortical cells where the nodule primordia forms and infection by rhizobia occurs (Kiss et al., 2009). In WT nodules, the vascular bundles are peripheral and the meristem is derived from the middle cortical cells (Xiao et al., 2014). Analysis of *lin* mutant nodules revealed that *lin* produces central vascular bundles, similar to those seen in lateral roots (Guan et al., 2013; Xiao et al., 2014). Endodermal reporter analysis showed that this is because of increased divisions in pericycle and endodermal cells in *lin* mutants, suggesting *LIN* may function to repress cell division of these cell types (Xiao et al., 2014).

### 1.7 Aims and objectives

Aladadi (2023) proposed that PUCK is involved in *Arabidopsis* radial growth, downstream of TDIF-PXY, controlling proliferation and pattern regulation. However, further characterisation of *PUCK* function is required to fully understand its role in secondary growth. The aim of this project was to better characterise *PUCK* to identify how and where it is functioning within the TDIF-PXY pathway. The objectives were to a) improve understanding of PUCK expression including its localisation, and b) define differences in the phenotype of *puck* mutants to try to elucidate the role of PUCK in controlling secondary growth. It was hypothesised that *PUCK* likely functions downstream of *CLE41* to balance cell division. The results from this work contribute to increasing understanding of the TDIF-PXY signalling pathway overall by identifying another unknown component and attempting to integrate it into the established network.

## 2.0 Materials and Methods

### 2.1 Plant materials and growth conditions

#### *2.1.1 Plant lines*

*Arabidopsis thaliana* Columbia ecotype Col-0 was used as wild-type (WT) in this study. *PUCKpro::GUS-GFP, puck, pxy,* and *pxy puck* lines were obtained from lab stocks (Table 1).

Table 1, The germplasm used in this MSc project and its source.

| Genotype | Details | Seed source |
|---|---|---|
| Wild-type | *Arabidopsis thaliana* Columbia ecotype Col-0 | NASC ID: N1093 |
| *pxy* | *pxy-3* | NASC ID: N9872 |
| *puck* | *puck-2* | (Aladadi, 2023) |
| *pxy puck* | Double mutant | (Aladadi, 2023) |
| *PUCKpro::GUS-GFP* | GUS expressed under the PUCK promoter | (Aladadi, 2023) |
| *35S::PUCK-EYFP* | PUCK overexpression line, 35S strong promoter, EYFP fluorescent protein tag for identifying subcellular localisation. | Generated here |

#### *2.1.2 1% MS agar plates*

When grown on plates, T2 generation seed was surface sterilised with 70% ethanol and stratified at 4 °C for 2-3 days in 0.1% agar solution before being sown onto 1% Murashige and Skoog (MS) medium (Duchefa, M0221) agar plates. Plates were sealed with micropore tape and placed in a climate-controlled growth chamber with 16h light at 21°C.

T1 generation seed with Kanamycin (Merck, 420311) plant resistance was surface sterilised with 5% bleach solution for no more than 5 minutes on a rocking table. In a flow hood 3-4 washes with 70% ethanol and 3 washes with sterile $H_2O$ were performed. Seed was then stratified for 2-3 days in 0.1% agar (Formedium, AGA03) solution and then sown onto 1% MS agar plates with 50 µg/mL Kanamycin for selection. Plates were sealed with micropore tape and placed in a climate-controlled growth chamber with 16h light at 21°C.

For growing on, 10cm pots were used with Levington Advance F2 plus sand, Melcourt peat free, John Innes 2, vermiculite and perlite soil mix (5:3:2:1:1). For T2, once germinated, 9 seedlings were transferred to each pot with the propagation lids on. For T1, transformants were identified as seedlings with green, expanded cotyledons and long roots. These were selected to be transferred to pots with 6-9 seedlings per pot with the propagation lids on. After 2-3 days, once plants had acclimated, the vents were opened and then gradually lids were removed. Plants were grown in a climate-controlled growth chamber with 16h light at 21°C.

*2.1.3 Soil*

When sowing straight to soil, T2 seed was stratified at 4°C for 2-3 days in 0.1% agar solution. Seed was then sown straight into 10 cm pots with Levington Advance F2 plus sand, Melcourt peat free, John Innes 2, vermiculite and perlite soil mix (5:3:2:1:1) with the propagation lids on to create high humidity. Plants were grown in a climate-controlled growth chamber with 16h light at 21°C. When the first true leaves emerged, the vents were opened and 2-3 days later, once plants had acclimated, the lids were removed. Plants were then thinned as necessary to ensure 9 plants per pot.

T1 seed with the BAR marker (phosphinothricin plant resistance) was sown into shallow trays with damp soil. Plants were grown in a climate-controlled growth chamber with 16h light at 21°C. As soon as seed had germinated, seedlings were sprayed with Basta (active ingredient phosphinothricin/glufosinate, 1 ml Basta per 400 ml $H_2O$) (ProGreen weed control solutions LTD, Kurtail Gold). In the case where Basta was not effective after 5 days, the concentration was increased to 3 ml per 400 ml $H_2O$, and seedlings sprayed daily. When the first true leaves emerged, the vents were opened and 2-3 days later, once plants had acclimated, the lids were removed. Transformants were transferred into pots with 6 seedlings per pot (soil mix: Levington Advance F2 plus sand, Melcourt peat free, John Innes 2, vermiculite and perlite soil mix (5:3:2:1:1)) to grow for collection of T2 seed for use in further experiments.

## 2.2 GUS staining and imaging of *PUCKpro::GUS-GFP* lines

*2.2.1 7-day-old seedlings*

*2.2.1.1 GUS staining*

GUS staining protocol followed according to Etchells et al. (2013). 7-day-old *PUCKpro::GUS-GFP* seedlings grown on 1% MS plates were harvested into 100 mM phosphate buffer (28 ml 200 mM $NaH_2PO_4$ (Melford, S23185-500.0), 72 ml 200 mM $Na_2HPO_4$ (Melford, S23100-500.0), 100 ml $ddH_2O$) on ice. Phosphate buffer was replaced with 90% acetone on ice for 5 minutes. 90% acetone was replaced with phosphate buffer on ice for 5 minutes. Phosphate buffer was replaced with fresh staining buffer (5 ml 100 mM phosphate buffer, 0.2 ml 10% triton-X, 0.1 ml 100 mM potassium ferrocyanide (Sigma, P3289-100G), 0.1 ml 100 mM potassium ferricyanide (Sigma, 702587-50G), 4.6 ml $ddH_2O$) for 10 minutes. Staining buffer was removed and staining buffer containing X-Gluc (Thermo Scientific, R0852) (0.2 ml 100 mM X-Gluc in 10 ml staining buffer) was added. Samples were incubated on the shaker in the 37 °C room overnight. The following day, the X-Gluc staining buffer was replaced with a 70% ethanol wash. The 70% ethanol was exchanged with fresh to remove chlorophyll and increase visibility of the GUS stain. Lines were observed at this stage to assess which had the best GUS expression and which were segregating.

*2.2.1.2 Microscopy*

For microscopy imaging, seedlings were transferred from 70% ethanol onto a watch glass with 80% glycerol and then transferred onto a microscope slide, mounted in 80% glycerol and a cover slip added. Imaging was performed using a Leica M165 FC Stereo microscope. Images were taken of 2-3 seedlings per line, recording GUS expression in various localisations of each seedling for qualitative analysis. Scale bars were added in ImageJ.

*2.2.2 5-week-old hypocotyls*

*2.2.2.1 GUS staining and embedding in Technovit*

5 GUS lines (n = 9 hypocotyls per line) were isolated from the plant and added to 100 mM phosphate buffer (28 ml 200 mM $NaH_2PO_4$, 72 ml 200 mM $Na_2HPO_4$, 100 ml $ddH_2O$) on ice. Phosphate buffer was replaced with 90% acetone on ice for 5 minutes. 90% acetone was replaced with phosphate buffer on ice for 5 minutes. Phosphate buffer was replaced with fresh staining buffer (5 ml 100 mM phosphate buffer, 0.2 ml 10% triton-X, 0.1 ml 100 mM potassium ferrocyanide, 0.1 ml 100 mM potassium ferricyanide, 4.6 ml $ddH_2O$) without X-Gluc for 10 minutes. A vacuum was pulled for

around 30 seconds to ensure the staining buffer infiltrated the tissues. Staining buffer was replaced with staining buffer containing X-Gluc (0.2 ml 100 mM X-Gluc in 10 ml staining buffer). Samples were incubated on the shaker in the 37 °C room overnight ready for infiltration the following day.

The following day the X-Gluc staining buffer was replaced with FAA (10 ml ethanol, 7 ml dd$H_2O$, 2 ml 37% formaldehyde, 1 ml acetic acid) for 30 minutes at room temperature on the shaker. FAA was replaced with 70% ethanol for 30 minutes at room temperature on the shaker. 70% ethanol was replaced with 85% ethanol for 30 minutes at room temperature on the shaker. 85% ethanol was replaced with 95% ethanol for 30 minutes at room temperature on the shaker. 95% ethanol was replaced with pre-infiltration solution (5 ml ethanol, 5 ml base liquid Technovit 7100 (Kulzer, 64709003)) for 90 minutes at room temperature on the shaker. Pre-infiltration solution was replaced with infiltration solution (0.1 g hardener, 10 ml base liquid Technovit 7100) which was incubated overnight at room temperature ready for polymerisation the following day.

The following day moulds were prepared. Polymerisation solution (15 ml infiltration solution, 1 ml Technovit 7100 hardener 2) was made. The embedding cavities were filled halfway with polymerisation solution, 2-3 hypocotyls were then positioned in each cavity before cavities were fully filled. Samples were polymerised for 2 hours at room temperature and then at 37 °C in the oven overnight. The following day samples were removed from 37 °C and left at room temperature to harden for approximately 1 week. Sample blocks were then removed from the mould and placed in tubes with desiccator beads for storage until sectioning.

*2.2.2.2 Microtome sectioning*

Sectioning was performed on the Micros RAZOR/STEELY Rotary Microtome with a glass knife and blade angle 5°. Sample blocks were trimmed with a razor blade and glued onto microtome stubs. Blocks were left to dry overnight before being further trimmed as needed prior to sectioning. 5 µm thick sections were taken in order to properly view the GUS stain. Once a section was cut, forceps were used to place it onto water on a slide on the slide warmer. Multiple sections from one block were added to each slide. Once the water had dried the samples were counterstained with 0.05% Ruthenium Red (Sigma Aldrich, R2751-1G) for 15 seconds. Slides were rinsed with water to remove

excess stain before being left on the slide warmer to dry. Slides were mounted with Histomount (National Diagnostics, HS-103) and a cover slip added. 5 lines were sectioned with n = 4-9 hypocotyls per line.

*2.2.2.3 Microscopy*

Slides were viewed using a Zeiss Axioskop light microscope with a colour camera to capture images of GUS expression localisation in the hypocotyl for qualitative analysis. Images were taken across 5 lines with n = 3-8 hypocotyls per line. Scale bars were added in ImageJ.

## 2.3 Histochemical staining and imaging of mutant lines

*2.3.1 Mutant lines and fixation*

WT, *puck, pxy,* and *pxy puck* mutants were grown to 6 weeks old for histochemical staining. Hypocotyls were isolated from plants and fixed overnight in 2.5% glutaraldehyde (Agar Scientific, R1011) in PBS to ensure that sectioning was performed at the same stage across all plants. The same hypocotyls were used for both phloroglucinol and aniline blue staining with n = 18 for WT and *pxy,* and n = 16 for *puck* and *pxy puck.*

*2.3.2 Vibratome sectioning*

*2.3.2.1 Vibratome preparation*

The Campden Model 7000smz was used for sectioning. A new stainless-steel blade was fitted and Opti-Cal alignment performed to ensure minimal Z-axis (vertical) errors. Ice was used around the water bath and dd$H_2O$ used in the water bath with the sample.

*2.3.2.2 Tissue preparation*

Fixed tissue was suspended in blocks of 5% agarose (Sigma, A9539-100G) for sectioning. 2-3 hypocotyls were placed inside a mould and melted agarose added. Samples were positioned centrally within the block and the agarose allowed to set. The blocks were then removed from the mould and trimmed down before being glued onto the adjustable vibratome mounts and the glue allowed to dry for approximately 15 minutes. Using the adjustable mounts allowed good transverse sections to be obtained

even if the sample was not perpendicular in the block. If required to store overnight between stains, samples in agarose blocks were removed from the vibratome mounts using a razor blade and placed in PBS. The next day, sample blocks were dried and glued onto the vibratome mounts once again, ready for sectioning.

*2.3.2.3 Vibratome sectioning*

Sample blocks were placed onto the magnetic patch in the water bath and the bath loaded onto the vibratome. For cutting, the vibratome was used at frequency: 75 Hz, amplitude: 1 mm, speed: 0.12 mm/s, and section thickness: 80-100 µm. Once cut, sections were moved onto a watch glass using a paintbrush. Approximately 3 sections were added to the watch glass for staining. Once stained, sections were moved onto a microscope slide for viewing and imaging.

*2.3.3 Phloroglucinol*

*2.3.3.1 Staining (Wiesner stain)*

To make Wiesner stain (phloroglucinol-HCl), 1 volume of concentrated HCl (37N) was mixed with 2 volumes of 3% phloroglucinol (Thermo Scientific, 24176100) solution (0.3 g in 10 ml of 70% ethanol). This stain must be prepared fresh. Once sections had been placed onto the watch glass, Wiesner stain was added for 5 minutes. Sections were then transferred onto a microscope slide and mounted in glycerol. Imaging must be performed relatively quickly once staining is complete since HCl will degrade the tissue.

*2.3.3.2 Microscopy and analysis*

Sections were observed and imaged using a Leica DM1500 LED brightfield microscope and camera. Scale bars were added in ImageJ.

Quantitative analysis was performed on the images to measure the radius of the xylem (mm), the number of lignified xylem cells in a 90° angle and the number of neighbours the xylem cell at the centre of the radial axis has. These parameters were used to quantify xylem production via xylem size and lignified xylem density, as well as xylem organisation across each genotype. If a phase two secondary growth ring was seen, this was excluded from counts. Measurements were performed in ImageJ. R was used for descriptive statistics, statistical tests and figures. Boxplots were generated for the xylem radius and the number of lignified xylem cells in a 90° angle, and a stacked bar

chart was generated for the number of neighbours the central xylem cell has. Shapiro-Wilk Normality Tests, histograms, Q-Q plots and Levene's Test for Homogeneity of Variances were used to dictate which statistical tests were performed, in order to identify whether there were any significant differences between the genotypes. For the xylem radius the data was normally distributed with equal variances and so an ANOVA with Tukey Multiple Comparisons of Means post-hoc test were performed. For the number of lignified xylem cells in a 90° angle, data was not normally distributed but with equal variances. Therefore, the non-parametric Kruskal-Wallace test with Pairwise Comparisons using Wilcoxon Rank Sum Test with Continuity Correction were performed. For the number of neighbours the central xylem cell has, count data is ordinal and so the Kruskal-Wallace test with Pairwise Comparisons using Wilcoxon Rank Sum Test with Continuity Correction were performed.

*2.3.4 Aniline blue*

*2.3.4.1 Staining*

To make 1% aniline blue solution, 1 g of aniline blue (Thermo Scientific, 401180250) was added to 100 ml 100 mM pH 7.9 Sorensen's phosphate buffer (5.4 ml 200 mM $NaH_2PO_4$, 94.6 ml 200 mM $Na_2HPO_4$). Once made, aniline blue stain can be stored in the dark at room temperature. Once sections had been placed onto the watch glass, aniline blue stain was added for 30 minutes in the dark. Sections were then washed with Sorensen's buffer before being transferred to a microscope slide. Sections were mounted in Sorensen's buffer and the cover slip sealed with nail varnish ready for imaging. Samples were kept in the dark as much as possible since aniline blue is light sensitive.

*2.3.4.2 Microscopy and analysis*

Imaging was performed using the Zeiss Apotome florescence microscope. The DAPI filter was used to visualise the fluorescence of the sample. When not in use the fluorescence shutter was closed to prevent sample bleaching. Images were taken down the eyepiece using an iPhone XS in order to obtain colour images showing the phloem stained with aniline blue as well as the autofluorescence of the lignin in the xylem. Scale bars were added in ImageJ.

Quantitative analysis was performed on the images to measure the width of the phloem band outside the xylem (mm) and the number of phloem cells within the xylem. These parameters were used to quantify phloem production via phloem size and vascular disorganisation via the level of intercalation of the phloem within the xylem across each genotype. If a phase two secondary growth ring was seen, this was excluded from counts. ImageJ was used for measurements. R was used for descriptive statistics, statistical tests and figures. A boxplot was generated for the phloem width, and a stacked bar chart was generated for the number of phloem cells within the xylem. Shapiro-Wilk Normality Tests, histograms, Q-Q plots and Levene's Test for Homogeneity of Variances were used to dictate which statistical tests were performed in order to identify whether there were any significant differences between the genotypes. For the phloem width, the data was not normally distributed with unequal variances. Therefore, the non-parametric Kruskal-Wallace test with Pairwise Comparisons using Wilcoxon Rank Sum Test with Continuity Correction were performed. For the number of phloem cells within the xylem, count data is ordinal and so the Kruskal-Wallace test with Pairwise Comparisons using Wilcoxon Rank Sum Test with Continuity Correction were performed.

## 2.4 Plant transformation

### *2.4.1 Overexpression construct*

A *35S::PUCK-EYFP* vector was ordered from VectorBuilder for generating a PUCK overexpression line and looking at subcellular localisation using EYFP. The *Escherichia coli* (*E. coli*) vector contained bacterial kanamycin resistance and plant phosphinothricin resistance (BAR marker).

### *2.4.2 Glycerol stocks*

For plates, 300 ml LB (Formedium, LMM0105) agar mix was melted in the microwave and once cool enough 300 µl kanamycin (50 mg/ml stock) was added to the mix and poured into petri dishes under sterile conditions. Once set, an inoculating loop was used to spread the VectorBuilder *E. coli* stock onto the plate. Plates were then placed in the 37 °C room overnight.

The following day, liquid cultures were generated. Under sterile conditions, 50 µl kanamycin (50 mg/ml stock) was added to 50 ml LB to make an LB stock. A sterile pipette tip was used to scrape a single colony from each petri dish and the tip was ejected into a universal tube containing 5 ml LB-kanamycin mix. The liquid culture was incubated on a rotor in the 37 °C room overnight. The following day, glycerol stocks were made. 700 µl overnight liquid culture was added to 700 µl sterile 80% glycerol, before being snap frozen in liquid nitrogen and placed in the -80 °C freezer.

*2.4.3 Miniprep*

With the remainder of the overnight liquid culture a Miniprep was performed using the Monarch Plasmid Miniprep kit (T1010L). Approximately 50 µl DNA elution buffer per tube was preheated to 50 °C. Aliquots of bacterial culture totalling 4.5 ml were added to a 2 ml Eppendorf and centrifuged at 16,000 g for 30 seconds after each aliquot was added. The supernatant was discarded. The pellet was resuspended by vortexing or pipetting in 200 µl resuspension buffer B1. After incubation at room temperature for 1 minute, 200 µl plasmid lysis buffer B2 was added and tubes inverted 5-6 times to mix. After incubation at room temperature for 1 minute, 400 µl plasmid neutralisation buffer B3 was added and tubes inverted until the colour neutralised. After incubation at room temperature for 2 minutes, the tubes were centrifuged at 16,000 g for 5 minutes. The supernatant was transferred to a spin column and centrifuged for 1 minute. The flow through was discarded before 200 µl plasmid wash buffer 1 was added. After centrifuging for 1 minute the flow through was discarded. 400 µl plasmid wash buffer 2 was added and tubes centrifuged for 1 minute. The column was then transferred to a clean 1.5 ml Eppendorf. 40 µl DNA elution buffer was added to the centre of the matrix before incubating at room temperature for 1 minute. The tubes were then centrifuged for 1 minute to elute the plasmid DNA. Plasmid DNA was stored at -20 °C.

*2.4.4 Nanodrop DNA concentration check*

A Nanodrop Spectrophotometer was used to check the concentrations of the isolated DNA. 0.5 µL of sample was used to measure the concentration (ng/µL) of DNA in each sample using the DNA-50 setting. dd$H_2O$ was used as the blank at the start of sample measurement.

*2.4.5 Whole plasmid sequencing*

The DNA concentration was used to calculate the volume of sample to send for sequencing. GENEWIZ was used to sequence the DNA of isolated plasmids. Benchling was used to analyse sequence results. The sequence from GENEWIZ match that of VectorBuilder.

*2.4.6 Agrobacterium transformation*

Competent cells (strain GV3101) were taken from the -80 °C freezer and melted on ice for 10 minutes. 5 µl plasmid DNA sample was added to competent cells and the tube was flicked gently to mix. Samples were kept on ice for 5 minutes. Samples were frozen in liquid nitrogen for 5 minutes and then samples were placed in the 37 °C heat block for 3-4 minutes. In sterile conditions, 300 µl LB was added and samples were shaken for 2 hours in the 30 °C room.

For plates, 200 ml LB agar mix was melted in the microwave and once cool enough 200 µl kanamycin (50 mg/ml stock) and 400 µl rifampicin (Thermo Scientific, J60836.03) (25 mg/ml stock) were added and plates poured. Once plates were set, 150 µl LB mix containing the plasmid DNA sample and competent cells was spread onto the plate under sterile conditions. Plates were then placed in the 30 °C room for 2 days. If agrobacterium cultures did not grow, the process was repeated spreading 200 µl LB mix on the plate instead.

After 2 days of agrobacterium growth on plates, liquid cultures were generated. A sterile pipette tip was used to scrape a single colony from each plate and the tip was ejected into a universal tube containing 10 ml LB, 10 µl kanamycin and 20 µl rifampicin. Tubes were incubated in the 30 °C room overnight. The following day, glycerol stocks were made. 700 µl overnight liquid culture was added to 700 µl sterile 80% glycerol before being snap frozen in liquid nitrogen and placed in the -80 °C freezer. The remainder of the overnight liquid culture was used to grow up for floral dipping. In the case where floral dipping was unsuccessful, glycerol stocks were used to re-grow liquid cultures in order to repeat the process.

*2.4.7 Floral dipping*

For floral dipping, 5 ml of overnight liquid culture was added to 250 ml LB containing 250 µl kanamycin and 500 µl rifampicin in a 500 ml flask. Flasks were placed on the shaker in the 30 °C room overnight. The following day the LB mix was transferred to centrifuge bottles before being centrifuged at 4,000 rpm for 15 minutes. The supernatant was discarded. Virkon (Rely On Lanxess, Camlab, 330013) was used to disinfect any solutions containing bacteria. Freshly made buffer (200 ml dd$H_2O$, 10 g sucrose (SLS, CHE3654) was added to the centrifuge bottled and the pellet resuspended by vortexing. Right before dipping, 40 µl Silwet L-77 (Fargro, De Sangosse, SLITH) was added. The culture was poured into a small container and wild-type plant flowers were dipped into the culture for 2 minutes. After 2 minutes, plants were placed on their side for 2 minutes to maintain humidity and prevent the culture mixture dripping onto and damaging the leaves. After dipping, plants were placed in trays with water and a propagation lid on to create high humidity, increasing transformation efficiency. Lids were removed after 2 days.

*2.4.8 Seed collection*

After floral dipping, plants were grown for seed collection. Once plants had bolted, inflorescence stems were tied up and plants placed into bags to prevent tangling with neighbouring plants and transgenic seed dispersal. Plants were watered until the siliques had filled, then left until dry. Seed was then collected from each plant. For transgenics containing the BAR marker, T1 seed was collected and post-ripened for 2 weeks before being sown in shallow trays. Once seed had germinated, trays were sprayed with Basta to select for phosphinothricin resistance. In the case of no transformants germinating the floral dipping process was repeated. Any transformants were transferred to pots to grow on and T2 seed collected for use in further experiments.

## 3.0 Results

### 3.1 Identification of *PUCK* tissue localisation using GUS staining

Although it was known that *puck* represses the *35S::CLE41* phenotype, it was unclear how or where *PUCK* functions to bring about this result. Histochemical β-Glucuronidase (GUS) staining uses the *E. coli* GUS gene as a qualitative reporter system to visually detect the tissue expression localisation of the gene to which GUS has been fused (Béziat et al., 2017). Identifying the localisation of a protein is useful to aid understanding of its function in space and time. In order to understand how *PUCK* functions in secondary growth, its tissue-specific expression localisation was elucidated to first identify where *PUCK* functions. This was used to help understanding of where *PUCK* may fit into the TDIF-PXY pathway.

6 independent *PUCKpro::GUS-GFP* lines (*PUCK::GUS,* KS1-6) were sown for analysis of 7-day-old seedlings and 5-week-old hypocotyls. Staining 7-day-old seedlings shows initial *PUCK* expression across the whole plant due to its small size. Checking for stain at this stage allows identification of which lines show strong expression and which are segregating or show no expression at all. Staining 5-week-old hypocotyls shows *PUCK* expression specifically across the vascular tissues during secondary growth (Etchells et al., 2013). KS1, KS2, KS4, KS5 and KS6 showed GUS expression in the 7-day-old seedlings grown on plates. Therefore, some seedlings of these lines were grown on in soil for analysis at 5 weeks. KS1 and KS5 showed GUS expression in all seedlings, whereas KS2, KS4 and KS6 were segregating, and KS3 showed no expression and so was not used for further analysis.

#### 3.1.1 7-day-old seedlings

At 7 days old, KS1, KS2, KS4, KS5 and KS6 seedlings were GUS stained. Seedlings were examined by eye and 2-3 per line were imaged using a Leica M165 FC Stereo microscope, to obtain further detail and ensure consistency of results (Figure 6A-D). Similar expression was seen across all individuals of all lines. Strong GUS expression was detected in the entirety of the first true leaves. Weaker signal was seen dotted across the cotyledons, but signal was not present in the cotyledon leaf veins. Signal strength in the hypocotyl varied between lines but expression was consistently present in all hypocotyls examined. Signal was also detected adjacent to the lateral root

meristem. In some seedlings, signal was seen in the centre of the root in the elongation and differentiation zones, however this was not consistent and therefore requires further investigation.

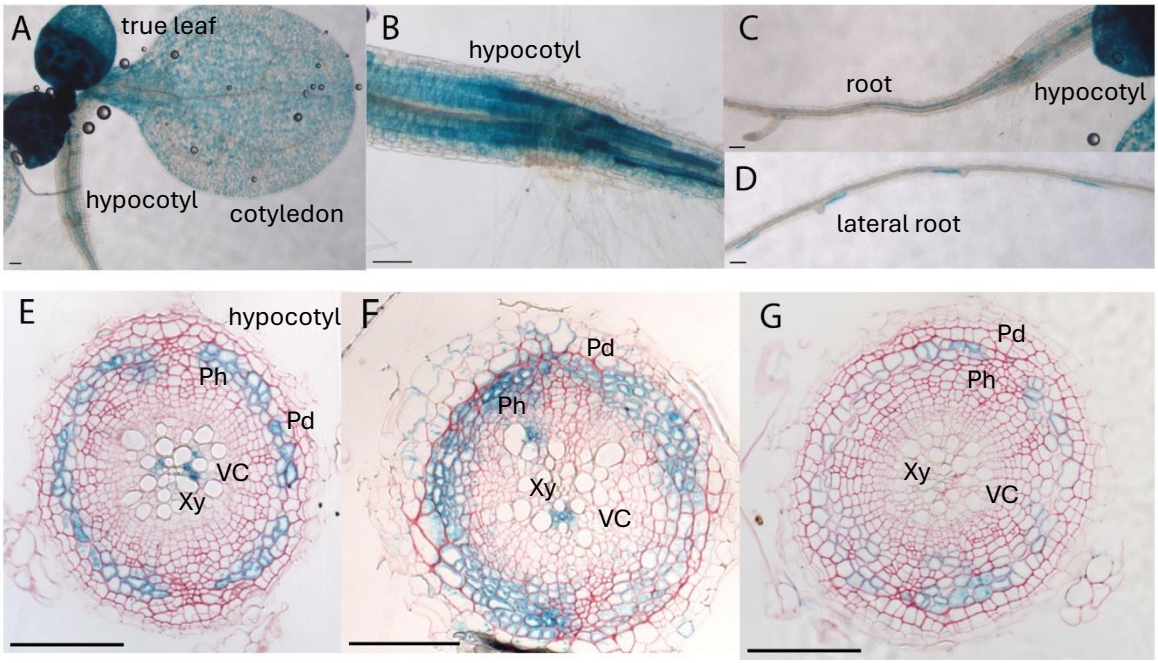


Figure 6, GUS staining of *PUCKpro::GUS-GFP*. 5 independent lines (KS1, KS2, KS4, KS5, KS6). A-D, 7-day-old seedlings. n=5 seedlings stained per line. 2-3 seedlings imaged per line. A, Leaf staining. B-C, Hypocotyl staining. D, Staining adjacent to the lateral root meristem. E-G, 5-week-old hypocotyls with Ruthenium Red counterstain. n=3-8 hypocotyls per line analysed. E, Representative image of expression across all lines. F, Showing GUS expression in the periderm. G, Showing GUS expression only in the phloem parenchyma. Xy marks xylem, VC marks vascular cambium, Ph marks phloem, Pd marks periderm. Scale bars 100 µm.

### 3.1.2 5-week-old hypocotyls

After growing for 5 weeks, KS1, KS2, KS4, KS5 and KS6 lines were analysed. Hypocotyls were isolated from the plant and, after GUS staining and embedding in Technovit, sections were counterstained with Ruthenium Red. Ruthenium Red stains the pectin in cell walls to provide contrast, making GUS localisation clearer (Chaffey et al., 2002). 3-8 hypocotyls per line were sectioned and stained to ensure consistency of results. Similar expression was seen across all individuals of all lines (Figure 6E-G). Strong GUS signal was detected in the phloem parenchyma across all hypocotyls in all lines. Signal was also seen in the differentiating xylem in some hypocotyls across all lines. In some hypocotyls, signal was also seen in the periderm, but this was not consistent.

### 3.1.3 Poplar: homologous gene expression localisation

When studying secondary growth, *Arabidopsis* is an excellent model due to the conservation of secondary thickening and genetic regulators with tree species such as the model tree, Poplar (Turley and Etchells, 2022). While in most cases *Arabidopsis* provides robust and reliable data, due to its size, higher resolution cambium transcriptomes are available in Poplar. Sundell et al. (2017) generated a Poplar transcriptome dataset from serial sections through the wood forming tissue and RNA sequencing of these sections. Transcriptome data can be useful to aid interpretation of tissue localisation data. Therefore, the Poplar dataset generated by Sundell et al. (2017) was examined to support the *Arabidopsis* GUS data generated in this study.

*Populus spp.* have several homologues of the *Arabidopsis PUCK* gene with varied expression localisations. The dataset generated by Sundell et al. (2017) shows that *Populus tremula* has seven *PUCK* homologues (Supplementary Figure 1). These expression patterns were compared with those of the *Arabidopsis PUCK::GUS* results from this study and two out of seven Poplar homologues appear to fit with the patterns seen in *PUCK::GUS* images (Figure 7) (Sundell et al., 2017). Potri.012G118600 showed the closest fit to *PUCK::GUS,* with the highest expression in the phloem, lower expression in the developing xylem and no expression in the cambium, as seen across all *Arabidopsis* GUS lines. Potri.015G117300 showed high expression in the phloem with expression decreasing to nothing across the cambium and developing xylem tissues, which could fit with some *Arabidopsis* GUS images showing phloem expression only.

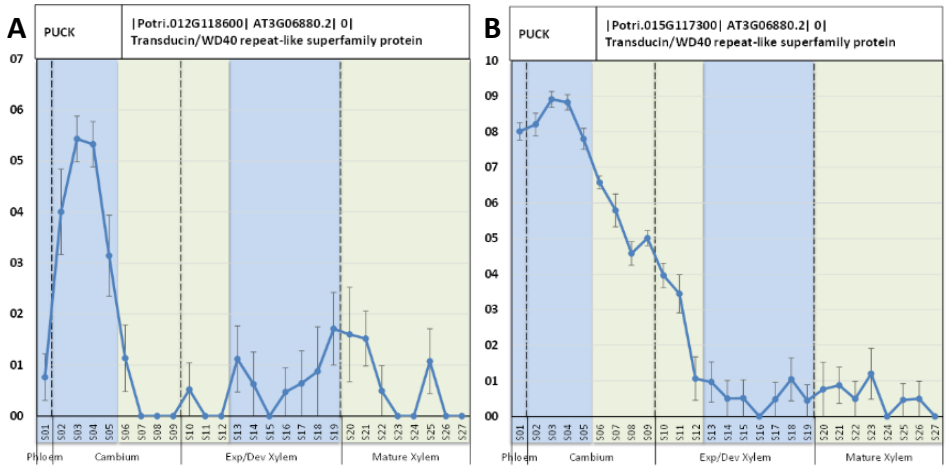


Figure 7, Expression patterns of two *Populus tremula* (Poplar) *PUCK* homologues, Potri.012G118600 and Potri.015G117300. A, Potri.012G118600 shows highest expression in the phloem, lower expression in the developing xylem and no expression in the cambium. B, Potri.015G117300 shows highest expression in the phloem with expression falling to zero across the cambium and developing xylem (Sundell et al., 2017). All seven Poplar homologue expression patterns can be found in Supplementary Figure 1.

### 3.1.4 *PUCK* single cell expression data

The Root Secondary Tissue single cell expression dataset, generated by Lyu et al. (2025), was compared to the *PUCK::GUS* localisation pattern from this study. It was found that the single cell and GUS data align. In the single cell expression dataset, the highest gene expression was shown to be in the mature phloem parenchyma, with lighter expression in the expanding xylem vessel as well as the young and maturing xylem parenchyma and periderm (Figure 8). This supports the strong GUS signal seen in the phloem parenchyma, and less consistent signal in the differentiating xylem and periderm tissues. The single cell data also showed no expression in the myrosin idioblast, non-conductive phloem parenchyma, companion cells, xylem fibres, late differentiating xylem vessels, mature xylem parenchyma or xylem vessel, which appears to align with the *PUCK::GUS* data. However, the single cell data did show very low expression in the vascular cambium which was not detected in the *PUCK::GUS* lines.

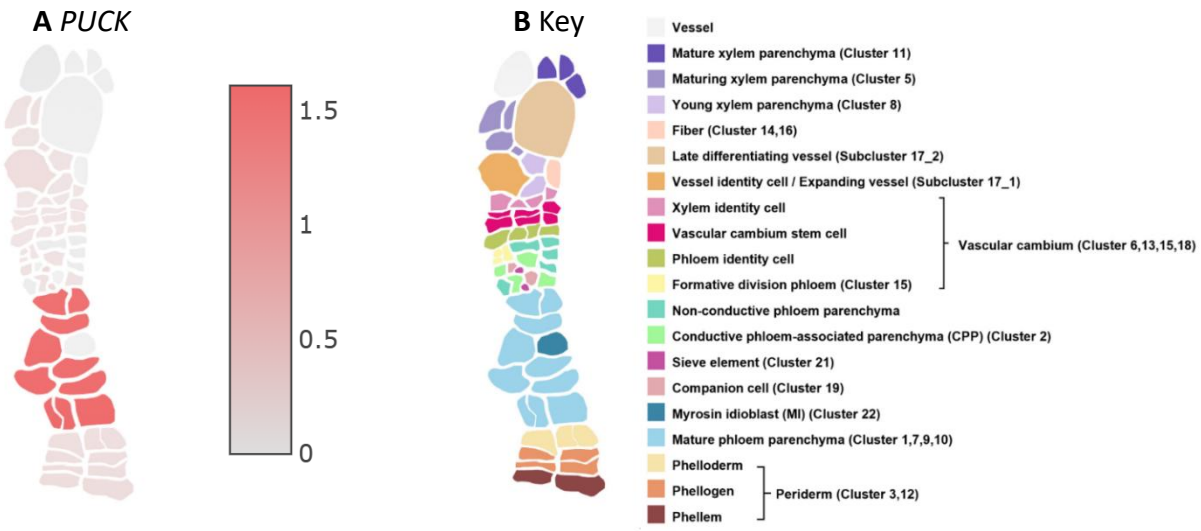


Figure 8, The Root Secondary Tissue single cell expression dataset. A, *PUCK* expression, with the level of expression indicated by the strength of red colour as per the legend. *PUCK* is expressed most strongly in the mature phloem parenchyma. There is also weaker expression in the expanding xylem vessel, and very weak expression in the periderm, phloem and xylem identity cells, young and maturing xylem parenchyma and vascular cambium stem cells. There is no expression in the myrosin idioblast, non-conductive phloem parenchyma, companion cells, xylem fibres, late differentiating xylem vessels, mature xylem parenchyma or xylem vessel. B, A key to indicate where each type of vascular tissue is on the diagram (Lyu et al., 2025).

## 3.2 Analysis of *puck* mutant hypocotyls using histochemical staining to identify how *PUCK* affects the vascular tissue

While the *35S::CLE41 puck* results showed that *puck* suppresses the *35S::CLE41* phenotype, the mechanism by which *PUCK* produces this result was not clear. Histochemistry is an incredibly useful tool for analysing specific cells within a tissue, or indeed components within a cell. Specific stains and imaging methods can be used to visualise unique cellular structures, allowing identification of cell type and localisation where this would otherwise be impossible to discern (Yadav et al., 2021). In order to identify how *PUCK* impacts secondary growth, cell-type specific stains were used on *puck* single and *pxy puck* double mutants to clearly visualise the effect of *puck* on the different cell types in the vascular tissue. This allowed identification of whether the changes in diameter and xylem tissue detected by Aladadi (2023) were associated with changes in vascular differentiation.

WT, *puck, pxy* and *pxy puck* lines (KS7-10) were grown and 6-week-old hypocotyls were isolated from the plants. Hypocotyls were embedded in agarose before being sectioned

using a vibratome. Sections were stained with phloroglucinol or aniline blue and imaged using light or fluorescence microscopy. Images were analysed in ImageJ and R to obtain quantitative results.

### 3.2.1 Staining for differentiated xylem localisation

Phloroglucinol-HCl (Weisner stain) stains the lignin in lignified xylem secondary cell walls. This allows visualisation of differentiated, mature xylem vessels in the hypocotyl using light microscopy. Images were taken and quantitative comparisons made between the genotypes (Figure 9).

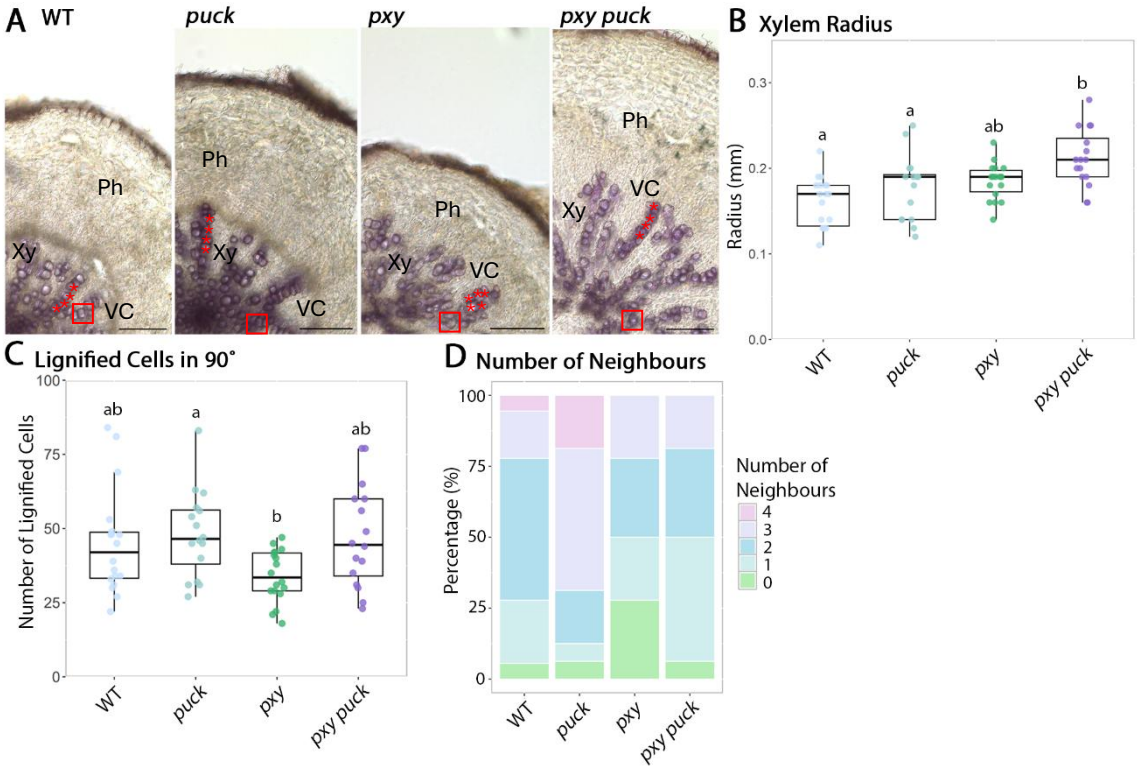


Figure 9, Phloroglucinol staining of 6-week-old hypocotyls from WT, *puck, pxy* and *pxy puck* mutant lines. n=16-18 hypocotyls per genotype. A, Images of stained transverse sections from each line using bright-field microscopy. Xy marks xylem, VC marks vascular cambium, Ph marks phloem. Red stars indicate cell files. Red box indicates an example of the central xylem cell for measuring the number of neighbours. Scale bars 100 µm. B, Boxplots to show the mean and standard deviation of the xylem radius (mm) across each genotype. ANOVA ($p = 0.000135$) and Tukey Multiple Comparisons of Means test were performed. C, Boxplots to show the median and IQR of number of lignified cells in a 90° segment of the xylem across each genotype. Kruskal-Wallis Rank Sum Test ($p = 0.0178$) and Wilcoxon Rank Sum Test with Continuity Correction were performed. D, A stacked bar chart to show the percentage of each number of neighbours the central xylem cell (halfway along the xylem radial axis) has across each genotype. Kruskal-Wallis Rank Sum Test ($p = 0.00661$) and Wilcoxon Rank Sum Test with Continuity Correction were

performed. Full statistical tables Supplementary Table 1, Supplementary Table 2, and Supplementary Table 3.

From the images, in WT, the lignified xylem vessels could be seen in cell files spanning out from the centre of the hypocotyl (Figure 9A). In many cases, two cell files could be seen running adjacent to one another. There were also occasional clumps of two to four or single lignified vessels present. The xylem tissue appeared to be a relatively consistent size and near circular in shape across all the WT hypocotyls.

In *puck,* the lignified xylem vessel organisation appeared to be only slightly disrupted compared to WT, however, there was definite variation between individual hypocotyls. While clear cell files could still be seen in most hypocotyls, groups or single lignified vessels were also present. These groups of vessels appeared to be around the edge of the xylem, closest to the cambium, with organisation becoming more similar to WT closer to the xylem centre. Two of the hypocotyls had very disrupted organisation, more similar to that seen in *pxy.* However, it is not clear why this phenotype was not consistent. Three of the hypocotyls had entered phase two of secondary growth, which was not seen in any other genotype, showing the high phenotypic variability in *puck*.

In *pxy,* organisation was clearly disrupted; there were xylem vessels visible which were not perpendicular to the horizontal plane and so appeared cut at oblique angles in some images. Cell files were disorganised with large groups as well as individual xylem vessels seen. *pxy* xylem tissue also seemed to be less circular overall. This phenotype is characteristic of a disrupted TDIF-PXY pathway.

In *pxy puck,* organisation seemed severely disrupted, similarly to in *pxy.* Xylem vessels were not perpendicular to the horizontal plane, appearing cut at oblique angles in many cases. Some cell files were present but many were disrupted with a large number of individual or clumps of xylem vessels seen. The xylem tissue overall seemed larger than that of WT and did not appear circular. There also seemed to be more space between lignified cells in *pxy puck* than in WT. To quantify these results, the images were analysed, graphs generated and statistical tests performed using R and ImageJ (Table 2).

Table 2, The quantitative measurements from images of phloroglucinol staining of the mature xylem vessels for WT, *puck*, *pxy* and *pxy puck* lines. n=16-18 hypocotyls per genotype. The xylem radius, number of lignified cells within a 90° segment and number of neighbours the central xylem cell had were

all recorded. Measurements were performed in ImageJ and statistical analysis performed in R. For the xylem radius, ANOVA (p = 0.000135) and Tukey Multiple Comparisons of Means test were performed. For the number of lignified cells within a 90° segment, Kruskal-Wallis Rank Sum Test (p = 0.0178) and Wilcoxon Rank Sum Test with Continuity Correction were performed. For the number of neighbours, Kruskal-Wallis Rank Sum Test (p = 0.00661) and Wilcoxon Rank Sum Test with Continuity Correction were performed. Full statistical tables Supplementary Table 1, Supplementary Table 2, and Supplementary Table 3.

| Genotype | Mean xylem radius (mm) (±standard deviation) | Median number of lignified cells in 90° (IQR) | Median number of neighbours (IQR) |
|---|---|---|---|
| WT | 0.16 (±0.029) | 42.0 (15.5) | 2.0 (0.75) |
| *puck* | 0.18 (±0.037) | 46.5 (18.3) | 3.0 (1.00) |
| *pxy* | 0.19 (±0.021) | 33.5 (12.8) | 1.5 (1.75) |
| *pxy puck* | 0.21 (±0.034) | 44.5 (26.0) | 1.5 (1.00) |

The radius of the xylem was measured in ImageJ from the centre to the median xylem edge per hypocotyl and the mean and standard deviation recorded across each genotype (Table 2). A boxplot was also generated to visualise the comparison between the genotypes (Figure 9B). This analysis suggested that WT had the smallest xylem radius of 0.16 mm and *pxy puck* had the widest at 0.21 mm. *pxy* had the least variation in xylem radius, whereas *puck* and *pxy puck* had the most variation. Statistical analysis was performed in R and recorded in Supplementary Table 1. The Shapiro-Wilk Normality Test showed that the data was normally distributed. A histogram and Q-Q plot were also used to visualise normality and supported the Shapiro-Wilk result. The Levene's Test for Homogeneity of Variance showed that the data had equal variances. This meant that a one-way ANOVA could be performed. The ANOVA showed that there was a significant difference in xylem width between the genotypes. A Tukey Multiple Comparisons of Means post-hoc test was performed to reveal which of the genotypes were significantly different. This showed that there were significant differences between WT and *pxy puck,* and between *puck* and *pxy puck,* suggesting that the double mutant *pxy puck* significantly affected the width of the xylem. Introducing the *puck* mutation into WT did not significantly affect the xylem width. However, introducing the *puck* mutation into *pxy* did significantly affect the xylem width compared to WT,

although not compared to *pxy* alone. This trend could suggest that *PUCK* may influence xylem production in conjunction with *PXY.*

The number of lignified cells in a 90° segment of the xylem was counted per hypocotyl and the median and interquartile range (IQR) recorded across each genotype (Table 2). A boxplot was also generated to visualise the comparison between the genotypes (Figure 9C). From this analysis it appeared that *pxy* had fewer lignified cells than all other genotypes at 33.5, with WT, *puck* and *pxy puck* having similar numbers of lignified cells (42.0-46.5). WT and *puck* had similar variation, with *pxy* having less variation and *pxy puck* having the most variation. Statistical analysis was performed in R and recorded in Supplementary Table 2. The Shapiro-Wilk Normality Test showed that the data was not normally distributed. This was supported by a histogram and Q-Q plot used to visualise normality. The Levene's Test for Homogeneity of Variance showed that the data had equal variances. However, since the data was not normal, a non-parametric test was used. The Kruskal-Wallis Rank Sum Test was performed and this showed that there was a significant difference in number of lignified cells between the genotypes. Pairwise Comparisons using the Wilcoxon Rank Sum Test with Continuity Correction was performed as the post-hoc test to reveal which of the genotypes were significantly different from one another. This showed that there were significant differences between *puck* and *pxy* only. This suggested that there was no real difference in the number of lignified cells between the genotypes as, based on the boxplot in Figure 9C, it could be argued that the interaction between *puck* and *pxy* in this parameter is additive. However, none of the mutants were significantly different to WT. From this parameter it is unclear how *puck* influences the xylem.

The number of neighbours that the central xylem cell has was recorded to quantify organisation. The xylem cell in the centre of the xylem radial axis was chosen, and the number of lignified neighbours that that xylem vessel had was recorded (Figure 9A). It was expected that in WT, it was most likely that this xylem vessel would have 2 neighbours either side of it in an organised cell file. Count data was recorded for this parameter to add up the number of hypocotyls with each number of neighbours per genotype (Table 2). A stacked bar chart was also generated to visualise the percentage of each number of neighbours the central xylem cell had between the genotypes (Figure 9D). This bar chart showed that WT had primarily 2 neighbours with some

variation (supporting the cell file hypothesis), *puck* had primarily 3 neighbours with some variation, and *pxy* and *pxy puck* had large variation suggesting organisation was altered in *pxy* and *pxy puck* mutants. Statistical analysis was performed in R and recorded in Supplementary Table 3. Since the data was ordinal, the Kruskal-Wallis Rank Sum Test was used to analyse the difference between the genotypes. This showed that there was a significant difference in the number of neighbours the central xylem cell had between the genotypes. Pairwise Comparisons using Wilcoxon Rank Sum Test with Continuity Correction was the post-hoc test performed to identify which of the genotypes were significantly different. This showed that there were significant differences between *puck* and *pxy,* and between *puck* and *pxy puck.* From these measurements it was unclear whether *puck* impacted xylem organisation, with the simplest explanation being that the *pxy puck* phenotype was a combination of *pxy* and *puck* single mutant phenotypes**.**

### 3.2.2 Staining for phloem localisation

Aniline blue stains the callose in phloem sieve plates, allowing identification of phloem localisation in the hypocotyl using fluorescence microscopy. Fluorescence microscopy also shows the xylem vessels, since the lignin in the xylem cell walls is autofluorescent. Lignin autofluoresces blue and callose fluoresces green using aniline blue staining, and so with this stain the organisation of the xylem and phloem tissues can be viewed relative to one another. This allowed intercalation and disorganisation of the vascular tissue to be detected. Images were taken and quantitative comparisons made between the genotypes (Figure 10).

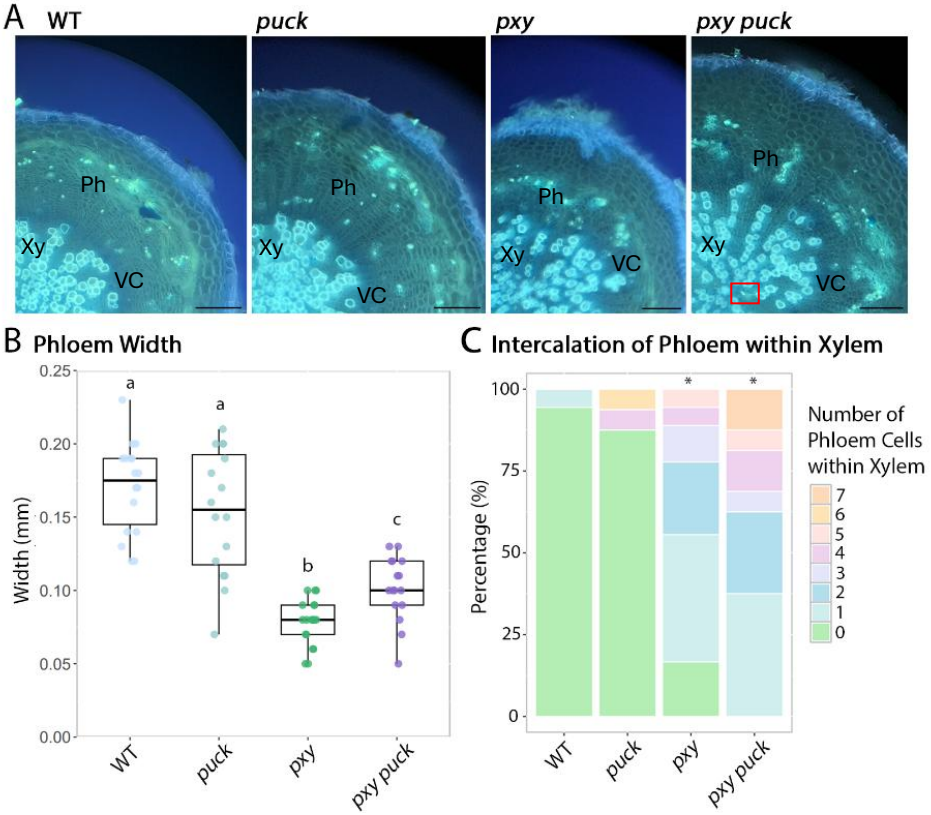


Figure 10, Aniline blue staining of 6-week-old hypocotyls from WT, *puck*, *pxy* and *pxy puck* mutant lines. n=16-18 hypocotyls per genotype. A, Images of stained transverse sections from each line using fluorescence microscopy. Xy marks xylem, VC marks vascular cambium, Ph marks phloem. Red box shows intercalation of phloem within the xylem. Scale bars 100 µm. B, Boxplots to show the median and IQR of the width of the phloem ring (mm) outside the xylem across each genotype. Kruskal-Wallis Rank Sum Test (p = 0.00363) and Wilcoxon Rank Sum Test with Continuity Correction were performed. C, A stacked bar chart to show the percentage of each number of phloem cells within the xylem (the level of intercalation) across each genotype. Asterisks indicate significant difference from WT. Kruskal-Wallis Rank Sum Test (p = 1.51e-08) and Wilcoxon Rank Sum Test with Continuity Correction were performed. Full statistical tables Supplementary Table 4, and Supplementary Table 5.

From the images, in WT, the phloem was spread broadly between the xylem and the periderm. Frequent green sieve plate fluorescence could be seen distributed across this area (Figure 10A). There was no intercalation of phloem within the xylem; the vascular tissues were produced on opposing sides of the vascular cambium.

In *puck,* the phloem was spread broadly between the xylem and periderm, similar to WT. There were 2 hypocotyls with narrower phloem bands and intercalation of phloem within the xylem, but this phenotype was not consistent.

In *pxy,* the phloem band was very narrow with concentrated sieve plate signals. There was also some intercalation of the phloem within the xylem. Vascular disorganisation is characteristic of a disrupted TDIF-PXY pathway.

In *pxy puck,* the phloem band was narrow with concentrated sieve plate signals, but appeared wider than in *pxy.* There was also consistent intercalation of the phloem within the xylem, more severely than that seen in *pxy.* To quantify these results, the images were analysed, graphs generated and statistical tests performed using R and ImageJ (Table 3).

Table 3, The quantitative measurements from images of aniline blue staining of the xylem and phloem using fluorescence microscopy for WT, *puck*, *pxy* and *pxy puck* lines. n=16-18 hypocotyls per genotype. The phloem width and level of intercalation were recorded. Measurements were performed in ImageJ and statistical analysis performed in R. For the phloem width, Kruskal-Wallis Rank Sum Test (p = 0.00363) and Wilcoxon Rank Sum Test with Continuity Correction were performed. For the level of intercalation, Kruskal-Wallis Rank Sum Test (p = 1.51e-08) and Wilcoxon Rank Sum Test with Continuity Correction were performed. Full statistical tables Supplementary Table 4, and Supplementary Table 5.

| Genotype | Median phloem width (mm) (IQR) | Median number of intercalated phloem within xylem (IQR) |
|---|---|---|
| WT | 0.18 (0.05) | 0 (0) |
| *puck* | 0.16 (0.08) | 0 (0) |
| *pxy* | 0.08 (0.02) | 1 (1) |
| *pxy puck* | 0.10 (0.03) | 2 (3) |

The width of the phloem band outside the xylem was measured per hypocotyl using ImageJ and the median and IQR recorded across each genotype (Table 3). In this parameter, any intercalation within the xylem tissue was not included. A boxplot was also generated to visualise the comparison of phloem width between the genotypes (Figure 10B). This analysis showed that WT had the largest phloem width of 0.18 mm, while the *pxy puck* phloem width of 0.10 mm was wider than the 0.08 mm of *pxy. puck* had the most variation in width, while *pxy* and *pxy puck* had less variation than WT. Statistical analysis was performed in R and recorded in Supplementary Table 4. The Shapiro-Wilk Normality test showed that the data was not normally distributed. A histogram and Q-Q plot were also used to visualise normality and supported the Shapiro-Wilk result. The Levene's Test for Homogeneity of Variance showed that the

variances were not equal. Therefore, since the data was not normal and had unequal variances, a non-parametric test was used. The Kruskal-Wallis Rank Sum Test was performed and this showed that there was a significant difference in the phloem width between the genotypes. Pairwise Comparisons using the Wilcoxon Rank Sum Test with Continuity Correction was performed as the post-hoc test to reveal which of the genotypes were significantly different from each other. This showed that there were significant differences between WT and *pxy,* WT and *pxy puck, puck* and *pxy, puck* and *pxy puck,* and between *pxy* and *pxy puck.* The trends seen in this parameter suggested that the interaction between *puck* and *pxy* is additive; *pxy puck* significantly altered phloem width compared to WT, *puck* or *pxy*. This pattern suggests that *PUCK* may repress phloem production.

The number of phloem cells within the xylem tissue was recorded per hypocotyl to quantify the level of intercalation, and the median and IQR recorded across each genotype. Count data was recorded for this parameter to add up the number of images with each number of intercalated phloem per genotype (Table 3). A stacked bar chart was also generated to visualise the percentage of each number of intercalated phloem between the genotypes (Figure 10C). This analysis showed that WT and *puck* had little to no intercalation, *pxy* had a range of levels of intercalation from 0 to 5, while *pxy puck* had a range of levels of intercalation from 1 to 7. Statistical analysis was performed in R and recorded in Supplementary Table 5. Since the data was ordinal, the Kruskal-Wallis Rank Sum Test was used to analyse the difference between the genotypes. This showed that there was a significant difference between the genotypes. Pairwise Comparisons using Wilcoxon Rank Sum Test with Continuity Correction was the post-hoc test performed to identify which of the genotypes were significantly different. This showed that there were significant differences between WT and *pxy,* WT and *pxy puck, puck* and *pxy,* and between *puck* and *pxy puck.* This suggested that *pxy* caused significant intercalation of phloem within the xylem. While there were higher levels of intercalation in *pxy puck* than *pxy* (with a high of 7 compared to 5 in *pxy*), this difference was not significant ($p = 0.23$). Therefore, it can be concluded that there is no significant difference between *pxy* and *pxy puck.* These results suggest that *PUCK* does not affect vascular organisation.

## 4.0 Discussion

### 4.1 What is the role of *PUCK* in secondary growth?

Vascular plants undergo secondary growth to increase structural support and nutrient transport to the growing tissues. This radial growth consists of increasing xylem and phloem production from the vascular cambium, which is controlled by the TDIF-PXY signalling pathway. Many downstream signalling components and transcription factors have been identified in regulating meristem maintenance and repression of vascular differentiation. However, there are gaps within the pathway preventing the full understanding of this key developmental process.

*PUCK* has been identified as a novel component of the TDIF-PXY signalling pathway. In this study, genetic characterisation of *PUCK* was performed in order to elucidate gene function and understand the role of *PUCK* in secondary growth. The initial mutagenesis screen by Aladadi (2023) showed that *puck* suppresses the *IRX3::CLE41* phenotype. Based on this result, it was hypothesised that *PUCK* likely functions downstream of *CLE41*, as a repressor of vascular differentiation. However, preliminary work attempting to elucidate gene function was inconclusive. Therefore, further gene characterisation experiments were performed with the aim of understanding where *PUCK* might fit into the TDIF-PXY signalling network. These experiments included GUS localisation and histochemical staining to show vascular cell types in *puck* and *pxy puck* mutants. Some key aspects of *PUCK* function have been characterised. It is now known that *PUCK* is localised to the phloem and xylem parenchyma in the hypocotyl, and that *PUCK* is a repressor of phloem differentiation.

### 4.2 *PUCK* localisation

In order to understand the role of a gene, it is important to identify where it functions in space and time. Expression analysis can be used to help clarify gene function if the localisation of gene expression overlaps with where an effect is seen in other phenotypic data such as mutant analysis. If the results support each other this increases confidence in the data.

Previous GUS reporter analysis did not appear to fit with the newly published *Arabidopsis* single cell sequencing dataset (Aladadi, 2023; Lyu et al., 2025). Therefore,

GUS reporter analysis was repeated, using the same lines generated by Aladadi (2023), to confidently elucidate *PUCK* tissue localisation. The results generated in this study are supported by the single cell sequencing data, as well as aligning with the Poplar transcriptome dataset and, therefore, were deemed robust (Sundell et al., 2017; Lyu et al., 2025). In seedlings, *PUCK* was primarily localised to the first true leaves, the hypocotyl, and adjacent to the lateral root meristem. In the hypocotyl of more mature plants, *PUCK* was expressed in the phloem and xylem parenchyma within the vascular tissue.

In GUS staining of 7-day-old seedlings, a variation in signal strength in the hypocotyl could be seen. This could be because some seedlings had initiated secondary growth and others had not, supporting the hypothesis that *PUCK* is involved in secondary growth regulation. Alternatively, variation in signal strength could be due to differences in the level of GUS expression across the lines. Analysis at multiple seedling ages, before and after initiation of secondary growth, could confirm whether *PUCK* expression strength is linked to secondary growth initiation. Staining the leaf tissue at a later stage would also be interesting to analyse how the expression of *PUCK* in the first true leaves might change over time. Signal detected adjacent to the lateral root meristem supports the hypothesis that PUCK functions in the TDIF-PXY pathway because PXY also functions in lateral root initiation (Cho et al., 2014). It would be interesting to investigate the role of *PUCK* in the root further, to understand why expression was adjacent to the lateral root, as well as why *PUCK* may have been present in the elongation and differentiation zones in some seedlings. It is unclear why the GUS signal was present in a dotted pattern across the cotyledons. However, since the signal seemed to be more concentrated at the leaf base, it would be interesting to test if this pattern followed the basiplastic gradient of cell cycling described by Donnelly et al. (1999). If so, is *PUCK* associated with cell division? There was no signal in the cotyledon leaf veins, suggesting *PUCK* does not function in primary growth of the vascular tissue.

The GUS localisation seen in 5-week-old hypocotyls supports the hypothesis that *PUCK* functions in differentiation of the vascular tissues. Although it cannot be ruled out, *PUCK* is not likely to be non-cell autonomous due to its large size. Therefore, it can be concluded that PUCK most likely functions within the differentiating xylem and phloem

tissues. The expression of *PUCK* in the phloem parenchyma fits with the fact that TDIF is produced in the phloem and translocates to the cambium. The expression of *PUCK* in the differentiating xylem parenchyma could be explained by the fact that the cambium organiser is a cell of xylem identity (Eswaran et al., 2024; Smetana et al., 2019). It would be interesting to investigate whether PUCK is involved in specifying organiser identity to developing xylem cells, or stem cell identity to cells in the cambium via promotion of CAIL TFs (Eswaran et al., 2024). However, the same gene functioning in the combination of phloem and xylem localisations is more difficult to interpret. Perhaps *PUCK* functions non-specifically in the differentiation process. Alternatively, *PUCK* could function in coordination of growth, including communication between the vascular and periderm tissues, allowing radial growth of all tissues to occur in sync. This would explain the inconsistent GUS signal detected in the phellogen. However, since the signal was not consistent, this suggested PUCK did not have an essential function in the phellogen at the 5-week stage of growth. Further work is required to confirm whether PUCK functions in the cork cambium. Overall, *PUCK* expression was localised to the phloem and xylem parenchyma of the hypocotyl. This localisation suggests that PUCK functions in differentiation of the vascular tissues.

Since the GUS and single cell expression data for *PUCK* align, the GUS results are likely to be robust. Both the single cell expression data and GUS expression showed that *PUCK* was expressed most highly in the mature phloem parenchyma (Lyu et al., 2025). Lower expression was found in the xylem vessels, xylem parenchyma and periderm, across both sources. However, in the single cell expression data, there appeared to be light *PUCK* expression in the cambium which was not present in the GUS images. It is unclear why this discrepancy was present, but since this expression was so low it can be concluded that the *PUCK::GUS* data is likely to be reliable.

The results of *PUCK::GUS* expression also seemed to fit with the Poplar transcriptome data. In Poplar, seven homologues of *PUCK* are present with varied expression patterns (Supplementary Figure 1) (Sundell et al., 2017). Two of these homologues, Potri.012G118600 and Potri.015G117300, had comparable expression patterns to those seen in the *Arabidopsis PUCK::GUS* lines. Potri.012G118600 showed the best fit with the *PUCK::GUS* expression pattern with the highest expression in the phloem, no expression in the cambium, and low expression in the xylem. Potri.015G117300

expression fit some of the GUS images, with highest expression in the phloem, and low expression in the cambium and xylem tissue. This suggested that *PUCK* may have homologous function between the *Arabidopsis* hypocotyl and the wood forming tissues of Poplar. However, the roles of the other 5 homologues with differing expression patterns to *Arabidopsis PUCK* remain unclear. The Poplar gene referenced in the dendrogram (Figure 5C), did not show any expression in the transcriptome data so it is unclear whether this homologue fits with the expression pattern of *Arabidopsis PUCK* (Sundell et al., 2017). Furthermore, the gene in Figure 5C refers to *Populus trichocarpa,* whereas the transcriptome dataset was generated from *Populus tremula* and so while these will be close homologues, the expression patterns could differ between species. Nevertheless, the key takeaway is that at least two of these homologues have expression patterns matching that of *Arabidopsis PUCK,* and so are likely to be present in the homologous Poplar TDIF-PXY pathway. It is interesting that *PUCK* is present as a single copy in *Arabidopsis,* since most *Arabidopsis* genes have multiple copies. Could these copies have been gained or lost between these two species across evolutionary time? Perhaps redundant copies gained new function in the *Medicago* homologue.

XVP is a NAC TF that activates xylem differentiation and promotes CLE44 transcription (Figure 3) (Yang et al., 2020a). The localisation of these XVP functions seems to fit with the results of *PUCK::GUS* expression; CLE44 transcription occurs in the phloem and xylem differentiation in the xylem parenchyma cells prior to vessel formation. Perhaps *PUCK* functions with XVP in some way. It would be interesting to generate a *puck xvp* double mutant in the first instance. If these results indicated a PUCK-XVP interaction, yeast-2-hybrid or co-immunoprecipitation experiments could be performed to analyse the proteins. Since XVP is a TF, it is able to translocate across cell types, however, how *PUCK* might interact with XVP across both the xylem and phloem requires further investigation. It could be that PUCK functions as a scaffold protein or in the endomembrane system to aid translocation of XVP between tissue types, in the same way as SHORTROOT (SHR) trafficking is promoted by SHR INTERACTING EMBRYONIC LETHAL (SIEL) in the endomembrane system (Wu and Gallagher, 2014).

### 4.3 The effect of *puck* on the vascular tissue

Generating a knockout mutant can help to identify what role the functional gene plays by assessing what is missing or disrupted in the mutant phenotype. In previous work, histochemical staining of *puck* mutant lines was performed using toluidine blue. This stain does not differentially stain the xylem and phloem, making it difficult to see the specific cell types in the vascular tissues and so results were inconclusive (Figure 5B). Therefore, analysis of the same lines generated by Aladadi (2023) was repeated using cell-type specific histochemical stains. This allowed visualisation of both the xylem and phloem cell types to more accurately analyse how *puck* mutants may affect the vascular tissue. Phloroglucinol was used to stain the mature xylem vessels and aniline blue was used to stain the phloem sieve plates. In the xylem, it was not clear whether *PUCK* functions to regulate xylem production. However, in the phloem it was concluded that *PUCK* functions to repress phloem differentiation.

For analysing the phloroglucinol staining of the xylem tissue, three parameters were assessed. Measuring the xylem width was chosen to assess the level of differentiation into xylem tissue. A greater width of lignified xylem suggests more differentiation to produce xylem tissue, encompassing xylem parenchyma as well as lignified vessels. From this parameter it was concluded that the xylem radius in *pxy puck* was significantly wider than WT or *puck.* Based on the pattern of the boxplot in Figure 9B, it could be suggested that *PUCK* may influence xylem production in conjunction with *PXY.*

Measuring the number of lignified cells in a 90° segment of the xylem was chosen to further assess the level of differentiation into mature xylem vessels. This quantified the production of lignified xylem vessels, not including the xylem parenchyma. A greater number of lignified cells suggests a greater rate of differentiation and more mature tissue, which could indicate premature differentiation. This parameter showed that there were no real differences between the number of lignified cells across the different genotypes. Since the width of *pxy puck* is significantly larger than WT while the number of lignified cells is not altered, it is possible that the number of xylem parenchyma cells is increased in the *pxy puck* mutant. However, it is also possible that the cell size is altered, or another cell type is affected and so further analysis is required to confirm this hypothesis. Overall, it can be concluded that the differences detected in xylem radius appear to be independent of xylem formation, and therefore, it is not likely that *PUCK* regulates xylem production.

The number of neighbours the central xylem cell has was chosen to quantify any organisational changes. In WT, xylem vessels are present in organised cell files spanning out from the centre of the hypocotyl, therefore, it was assumed that in WT, there would be clear cell files meaning there was 1 neighbour either side of the chosen cell, with some natural variation expected. The central xylem cell was selected because it was hypothesised that the vessel in the centre of a cell file would adequately show whether a file was disorganised or not. However, this hypothesis did not consider that there are often two cell files adjacent to each other. Furthermore, measuring the neighbours of one xylem vessel from each image did not provide a very high n for analysis and so these results do not have a very high confidence. However, counting multiple xylem vessels from the same image leads to pseudo stratification and complex statistical considerations. Overall, the spread of results in WT does seem to fit what was expected; around 50% of WT had two neighbours with an even variation of less or more neighbours either side of this. However, the mutants did not show conclusive significant differences from WT. This may be because the recording method did not effectively quantify organisational changes. For example, clumps of three xylem vessels were recorded as two neighbours which is the same as if the vessel was in a cell file. It could also be because more differences were seen at the edge of the xylem closer to the cambium, so selecting the central xylem cell would not pick up those differences. Overall, organisational changes were not observed between these genotypes using the parameters measured here. As such there is no evidence to suggest that *PUCK* influences xylem organisation.

For the xylem tissue, the number of lignified cells and the number of neighbours did not show a significantly different pattern across the genotypes. These results support the hypothesis that *PUCK* does not impact xylem differentiation. However, three *puck* hypocotyls had secondary growth rings not seen in any of the other genotypes, suggesting *PUCK* may have a role in controlling the transition to secondary growth. Furthermore, it is interesting that the localisation of *PUCK* expression in the xylem parenchyma coincides with the localisation where the *pxy puck* mutant width shows the greatest difference from WT. One hypothesis for this is that *PUCK* functions to balance differentiation via influencing cell fate decisions. This could explain why *PUCK* is present in both the differentiating xylem and phloem tissue. While signalling

components upstream of TDIF are localised to the phloem, it is also interesting to note that the cambium stem cell organiser is a cell of xylem identity, which could help to explain the presence of PUCK in the xylem (Eswaran et al., 2024). The largest effect on the vascular tissue was seen when analysing the phloem, which fits with the result that the strongest GUS signal was detected in the phloem parenchyma. Not all hypocotyls analysed showed *PUCK::GUS* expression in the xylem and this could explain why the effects of *puck* on the xylem were less evident.

For analysing the aniline blue staining of the phloem tissue, two parameters were assessed. The phloem width was selected to assess the level of differentiation and rate of phloem production across the mutant lines. A wider phloem suggests more differentiation to produce phloem tissue. When studying this parameter, significant differences were found between *puck, pxy* and *pxy puck,* with WT being significantly different from *pxy* and *pxy puck.* Based on the pattern seen in Figure 10B, it is likely that the interaction between *puck* and *pxy* is additive. This pattern of additive phenotype suggests that PUCK functions to repress phloem differentiation; with *puck* mutated there was more phloem in *pxy puck* than *pxy,* meaning functional *PUCK* represses phloem production. However, *puck* single mutants did not show a significant difference to WT; it could be hypothesised that PUCK functions to balance differentiation of vascular tissues via influencing cell fate decisions.

Since aniline blue staining is imaged using fluorescence microscopy, and the xylem is autofluorescent, this allowed the xylem and phloem to be viewed relative to one another. The level of intercalation was used to assess whether vascular organisation was affected by *puck* mutants. In WT, phloem is produced outside the xylem on opposing sides of the vascular cambium. If there is intercalation of phloem within the xylem this is indicative of disrupted signalling in the vascular cambium. The number of phloem cells within the xylem was recorded to quantify this parameter. The more phloem fluorescence signals detected within the xylem tissue, the greater the disorganisation. From this parameter it was concluded that *pxy* significantly disrupts vascular organisation. When the TDIF-PXY pathway is disrupted, the vascular tissue becomes disorganised. There is no significant difference between *pxy* and *pxy puck* ($p = 0.23$). The disorganisation in the vascular tissue is maintained in this double mutant. Perhaps the increased radius of *pxy puck* detected when measuring the xylem is due to

this disorganisation, with phloem tissue displacing some of the xylem tissue. Overall, it is hypothesised that PUCK could be a scaffold protein involved in repressing phloem differentiation. This is supported by the expression data showing the strongest *PUCK* expression in the phloem parenchyma. Increased phloem differentiation may protect plants from disrupted vascular organisation in *35S:CLE41 puck* lines.

## 4.4 Homologues of PUCK: LIN in *Medicago*

In an attempt to better understand *PUCK* function, a homology search was performed. *LIN* was identified as a homologue of *PUCK* in *Medicago truncatula* (Figure 5C). *LIN* is known to be required for regulating rhizobial colonisation and nodule differentiation from primordia in the formation of root nodules (Kiss et al., 2009; Kuppusamy et al., 2004). *lin* mutants displayed central vascular bundles, compared with the peripheral vascular bundles of WT root nodules (Xiao et al., 2014). Xiao et al. (2014) suggested that *LIN* may function to repress cell division of pericycle and endodermal cells. Could this control of proliferation be a role for *LIN* homologues in non-leguminous species? Liu et al. (2021) found that LIN has auto-ubiquitination activity and is localised to the trans-Golgi network and early endosome (TGN/EE), suggesting that LIN functions in membrane trafficking.

Kiss et al. (2009) aligned LIN to multiple homologues from closely related plant species (Figure 11). However, low similarity was found between LIN and *Arabidopsis* proteins in comparison to the other plant species analysed. There was not one *Arabidopsis* sequence which shared all the homologous domains of LIN. The WD40 domains and armadillo repeats were conserved between LIN and PUCK, however, LIN also contains a U-box domain with E3 ubiquitin ligase activity (Kiss et al., 2009). This U-box domain was conserved between LIN and At1G23030. Considering the differences between PUCK and LIN in both sequence and organism, it is unclear what the function of PUCK could be. It was suggested that the WD40 and Armadillo repeat regions in LIN may control target specificity or post-translational modifications (Kiss et al., 2009). It is possible that this function is conserved in PUCK. PUCK is larger than LIN, with no U-box domain, and both proteins consist of large regions of unknown function. Understanding these regions may help to better characterise the role of these proteins. Since homologous sequences to LIN are present in non-legume species, the LIN

domains cannot uniquely be involved in nodulation, but it is unclear what function these homologous genes may have (Kiss et al., 2009). Considering LIN affects the localisation of nodule vasculature it is not surprising that PUCK seems to be involved in *Arabidopsis* vascular development (Xiao et al., 2014). Perhaps this system has been co-opted from the plant defence pathway, where several U-box E3 ligases have been identified (Kiss et al., 2009).

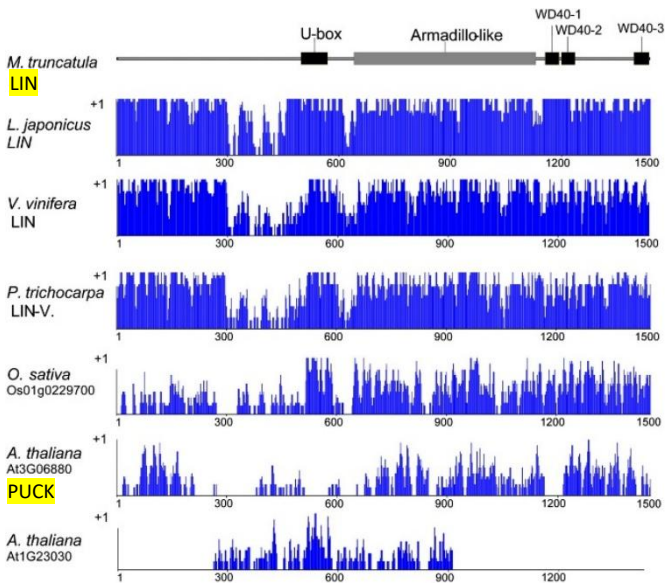


Figure 11, Results of alignment of the *M. truncatula* LIN protein with its closest plant homologues. The top line shows a schematic of the *M. truncatula* LIN protein with the locations of the U-box, Armadillo, and WD40 domains. Below shows a graphical representation of the similarity of LIN to its closest plant homologues, where 1 is an identical residue (Kiss et al., 2009). Highlighted labels show LIN and PUCK alignment.

Upon further investigation into LIN, it was found that it interacts with VAPYRIN (VPY) and EXO70H4 to control polar growth of infection threads during nodulation (Liu et al., 2019). Since the protein-protein interaction domains are conserved between LIN and PUCK, it is fair to assume that PUCK does not act alone (Liu et al., 2019). Characterisation of other PUCK homologues could help to discern a conserved function. Possessing protein-protein interaction domains could account for the varied phenotypes observed in mutant studies (Stone et al., 2007). Elucidation of PUCK's interacting partners through a proximity labelling experiment, for example, is crucial to confidently identifying its function.

A recent paper on *Medicago* by Teyssendier de la Serve et al. (2025) has revealed that *MtCLE37* is required to promote nodulation and increase root stele diameter upon rhizobium inoculation. This *MtCLE37* has been named symbiotic nodulation TDIF

(sTDIF) and uncovers a novel function of TDIF signalling peptides. The increases in root stele diameter occur via production of an increased number of vascular cells (Teyssendier de la Serve et al., 2025). It is already known that *PXY* functions in the *Arabidopsis* lateral roots, however, this research suggests that a TDIF-PXY signalling system could be conserved in *Medicago* and involved in regulating nodulation (Cho et al., 2014; Teyssendier de la Serve et al., 2025). *stdif* mutants showed reduced nodule number and no increase in root stele diameter upon rhizobium inoculation. This suggests that sTDIF is required for the increase in vascular cells allowing greater root stele diameter for nodule formation (Teyssendier de la Serve et al., 2025). Could sTDIF function with LIN in the same way as TDIF might function with PUCK in the vascular tissue? Or, could studying sTDIF in nodulation aid understanding of the TDIF-PXY pathway overall? Further investigation into this new signalling system is required to answer these questions.

### 4.5 The role of *PUCK* in secondary growth

Overall, the results of this study support the initial hypothesis that *PUCK* likely functions downstream of *CLE41,* in the TDIF-PXY pathway to control secondary growth (Figure 12). The aim of better characterising *PUCK* function has been achieved. The phloem localisation and the *puck* mutant results suggest that *PUCK* may function directly downstream of *CLE41*, potentially involved in synthesis and maturation of TDIF. However, this would not explain the presence of *PUCK* in the xylem; it is unclear how *PUCK* can function in both the xylem and phloem. It could be that *PUCK* has two independent functions, or, although unusual for a protein of this size, acts non-cell autonomously by translocating between the two localisations via mRNA or unfolding and refolding. Accounting for all results from this project, it is proposed that that *PUCK* may be a scaffold protein involved in influencing cell fate decisions resulting in repression of phloem differentiation. However, where PUCK fits into the TDIF-PXY pathway remains unknown. Further characterisation of *PUCK* function is required to fully understand how this gene contributes to control of vascular organisation and differentiation.

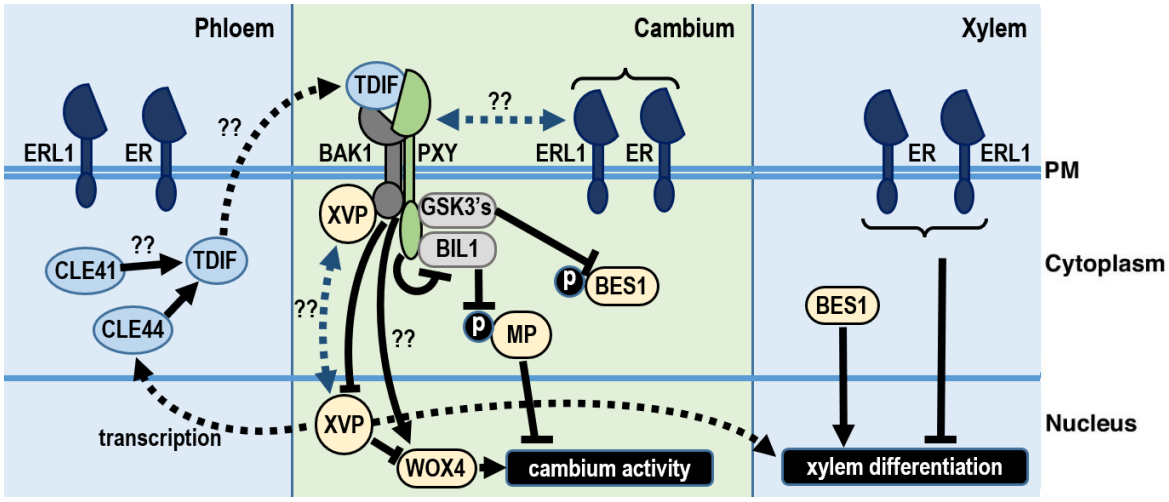


Figure 12, A diagram showing the localisation and putative downstream components of TDIF-PXY signalling in the phloem, cambium and xylem. The nucleus, cytoplasm and plasma membrane (PM) are labelled. Blue bubbles show PXY ligand components, yellow bubbles show transcription factors, grey bubbles show GSK3s, RLKs are within the PM. Arrows indicate positive interaction, blunt arrowheads indicate inhibition, dotted arrows indicate translocation. Question marks show where knowledge is missing within the network. (This includes how CLE41 produces TDIF, how TDIF translocates to the cambium, what triggers XVP to translocate to the nucleus, and limited evidence for a PXY-ER interaction). P indicates phosphorylation. From the results of this thesis, it is clear *PUCK* is not expressed within the cambium. Where exactly PUCK fits into the signalling network has not been identified. It is possible PUCK functions in synthesis and maturation of TDIF in the phloem, or involved in translocating XVP between the phloem and xylem. Adapted from (Bagdassarian et al., 2020).

## 4.6 Future work

To more clearly interpret the *puck* mutant results, the *35S::PUCK-EYFP* overexpression line requires analysis. The opposite phenotype to *puck* could allow clarification of the role of *PUCK* in the vascular tissue. This line could also be used to identify the subcellular localisation of *PUCK* using the EYFP tag. Data from Eswaran et al. (2024) shows that *PUCK* expression is reduced in the *pxy* mutant and increased in the *35S::CLE41* overexpression line. Crossing a PUCK reporter into these backgrounds could show the localisation of these changes to more conclusively identify whether *PUCK* acts downstream of *CLE41*. Further research into the function of *PUCK* homologues could also shed light on a conserved function across related plant species. A proximity labelling experiment using the TurboID tag may increase understanding of gene function by identifying its interacting partners, while also identifying more novel components of the TDIF-PXY signalling pathway or integration of existing components.

As well as the previously mentioned *puck xvp* mutant line, there are other double mutant lines which could prove useful in understanding *PUCK* function. Based on the localisation data, generation of a *cle41 puck* mutant could be interesting as this may aid interpretation of where *PUCK* may function relative to TDIF within the pathway (Figure 12). While preliminary studies suggest that *puck* does not interact with *er*, a *pxy puck er* triple mutant would be interesting to identify whether ER performs any compensatory function in the *pxy puck* mutant (Aladadi, 2023). A *lbd4 puck* double mutant could also be useful to identify how *PUCK* impacts phloem production, and how it might fit into the signalling network.

It is known that phytohormones interact with the TDIF-PXY pathway (Brackmann et al., 2018; Etchells et al., 2012; Han et al., 2018; Hirakawa et al., 2010). It would be interesting to test how *PUCK* is affected by these phytohormones. This could include how *PUCK* expression varies after different phytohormone treatments, as well as using *PUCK* reporter lines to identify any alterations to *PUCK* localisation due to hormone changes. Mass spectrometry could also be used to measure the levels of multiple different hormones across different *puck* mutant lines (Pan et al., 2010).

There are still many aspects of TDIF-PXY signalling yet to be identified, including generation and exportation of TDIF, the influence of PXY on the identity of cells leaving the cambium, and coordinating downstream signal transduction factors and transcriptional targets (Etchells et al., 2016). Further characterisation of *PUCK* aims to aid elucidation of this complex signalling mechanism. A more complete TDIF-PXY pathway would increase understanding of secondary growth control. This is key to being able to increase plant biomass and manipulate wood production, providing an increased source of paper, building materials and most importantly biofuel which is crucial in the current climate crisis (Aladadi, 2023; Stephenson et al., 2014). Aside from wood production, secondary growth manipulation could also allow greater reallocation of resources or increased stem stability under environmental stress. Broader research topics for future work include identifying conservation of biomass deposition in monocots, regulation of vascular development under stress, and considering the impact of genetic redundancy on secondary growth in trees (Turley and Etchells, 2022).

## 5.0 References


Agusti, J., Herold, S., Schwarz, M., Sanchez, P., Ljung, K., Dun, E. A., Brewer, P. B., Beveridge, C. A., Sieberer, T., Sehr, E. M., et al. (2011). Strigolactone signaling is required for auxin-dependent stimulation of secondary growth in plants. *Proc. Natl. Acad. Sci.* 108, 20242–20247.

Aladadi, W. (2023). Characterisation of new genes involved in *Arabidopsis* vascular development. Durham University. PhD Thesis.

Bagdassarian, K. S., Brown, C. M., Jones, E. T. and Etchells, P. (2020). Connections in the cambium, receptors in the ring. *Curr. Opin. Plant Biol.* 57, 96–103.

Baima, S., Possenti, M., Matteucci, A., Wisman, E., Altamura, M. M., Ruberti, I. and Morelli, G. (2001). The Arabidopsis ATHB-8 HD-Zip Protein Acts as a Differentiation-Promoting Transcription Factor of the Vascular Meristems. *Plant Physiol.* 126, 643–655.

Béziat, C., Kleine-Vehn, J. and Feraru, E. (2017). Histochemical Staining of β-Glucuronidase and Its Spatial Quantification. In *Plant Hormones* (ed. Kleine-Vehn, J.) and Sauer, M.), pp. 73–80. New York, NY: Springer New York.

Brackmann, K., Qi, J., Gebert, M., Jouannet, V., Schlamp, T., Grünwald, K., Wallner, E.-S., Novikova, D. D., Levitsky, V. G., Agustí, J., et al. (2018). Spatial specificity of auxin responses coordinates wood formation. *Nat. Commun.* 9, 875.

Carlsbecker, A., Lee, J.-Y., Roberts, C. J., Dettmer, J., Lehesranta, S., Zhou, J., Lindgren, O., Moreno-Risueno, M. A., Vatén, A., Thitamadee, S., et al. (2010). Cell signalling by microRNA165/6 directs gene dose-dependent root cell fate. *Nature* 465, 316–321.

Chaffey, N., Cholewa, E., Regan, S. and Sundberg, B. (2002). Secondary xylem development in *Arabidopsis* : a model for wood formation. *Physiol. Plant.* 114, 594–600.

Cho, H., Ryu, H., Rho, S., Hill, K., Smith, S., Audenaert, D., Park, J., Han, S., Beeckman, T., Bennett, M. J., et al. (2014). A secreted peptide acts on BIN2-mediated phosphorylation of ARFs to potentiate auxin response during lateral root development. *Nat. Cell Biol.* 16, 66–76.

Coates, J. (2003). Armadillo repeat proteins: beyond the animal kingdom. *Trends Cell Biol.* 13, 463–471.

Denis, E., Kbiri, N., Mary, V., Claisse, G., Conde E Silva, N., Kreis, M. and Deveaux, Y. (2017). *WOX 14* promotes bioactive gibberellin synthesis and vascular cell differentiation in Arabidopsis. *Plant J.* 90, 560–572.

Donnelly, P. M., Bonetta, D., Tsukaya, H., Dengler, R. E. and Dengler, N. G. (1999). Cell Cycling and Cell Enlargement in Developing Leaves of Arabidopsis. *Dev. Biol.* 215, 407–419.

Emery, J. F., Floyd, S. K., Alvarez, J., Eshed, Y., Hawker, N. P., Izhaki, A., Baum, S. F. and Bowman, J. L. (2003). Radial Patterning of Arabidopsis Shoots by Class III HD-ZIP and KANADI Genes. *Curr. Biol.* 13, 1768–1774.

Eswaran, G., Zhang, X., Rutten, J. P., Han, J., Iida, H., López Ortiz, J., Mäkilä, R., Wybouw, B., Planterose Jiménez, B., Vainio, L., et al. (2024). Identification of cambium stem cell factors and their positioning mechanism. *Science* 386, 646–653.

Etchells, J. P. and Turner, S. R. (2010a). The PXY-CLE41 receptor ligand pair defines a multifunctional pathway that controls the rate and orientation of vascular cell division. *Development* 137, 767–774.

Etchells, J. P. and Turner, S. R. (2010b). Orientation of vascular cell divisions in Arabidopsis. *Plant Signal. Behav.* 5, 730–732.

Etchells, J. P., Provost, C. M. and Turner, S. R. (2012). Plant Vascular Cell Division Is Maintained by an Interaction between PXY and Ethylene Signalling. *PLoS Genet.* 8, e1002997.

Etchells, J. P., Provost, C. M., Mishra, L. and Turner, S. R. (2013). *WOX4* and *WOX14* act downstream of the PXY receptor kinase to regulate plant vascular proliferation independently of any role in vascular organisation. *Development* 140, 2224–2234.

Etchells, J. P., Smit, M. E., Gaudinier, A., Williams, C. J. and Brady, S. M. (2016). A brief history of the TDIF-PXY signalling module: balancing meristem identity and differentiation during vascular development. *New Phytol.* 209, 474–484.

Fisher, K. and Turner, S. (2007). PXY, a Receptor-like Kinase Essential for Maintaining Polarity during Plant Vascular-Tissue Development. *Curr. Biol.* 17, 1061–1066.

Gaillochet, C. and Lohmann, J. U. (2015). The never-ending story: from pluripotency to plant developmental plasticity. *Development* 142, 2237–2249.

Gandotra, N., Coughlan, S. J. and Nelson, T. (2013). The Arabidopsis leaf provascular cell transcriptome is enriched in genes with roles in vein patterning. *Plant J.* 74, 48–58.

Ghosh, S., Nelson, J. F., Cobb, G. M. C., Etchells, J. P. and De Lucas, M. (2022). Light regulates xylem cell differentiation via PIF in Arabidopsis. *Cell Rep.* 40, 111075.

Goodstein, D. M., Shu, S., Howson, R., Neupane, R., Hayes, R. D., Fazo, J., Mitros, T., Dirks, W., Hellsten, U., Putnam, N., et al. (2012). Phytozome: a comparative platform for green plant genomics. *Nucleic Acids Res.* 40, D1178–D1186.

Gu, Y. and Innes, R. W. (2012). The KEEP ON GOING Protein of *Arabidopsis* Regulates Intracellular Protein Trafficking and Is Degraded during Fungal Infection. *Plant Cell* 24, 4717–4730.

Guan, D., Stacey, N., Liu, C., Wen, J., Mysore, K. S., Torres-Jerez, I., Vernié, T., Tadege, M., Zhou, C., Wang, Z., et al. (2013). Rhizobial Infection Is Associated with the

Development of Peripheral Vasculature in Nodules of *Medicago truncatula*. *Plant Physiol.* 162, 107–115.

Han, S., Cho, H., Noh, J., Qi, J., Jung, H.-J., Nam, H., Lee, S., Hwang, D., Greb, T. and Hwang, I. (2018). BIL1-mediated MP phosphorylation integrates PXY and cytokinin signalling in secondary growth. *Nat. Plants* 4, 605–614.

Hilleary, R. and Gilroy, S. (2018). Systemic signaling in response to wounding and pathogens. *Curr. Opin. Plant Biol.* 43, 57–62.

Hirakawa, Y., Shinohara, H., Kondo, Y., Inoue, A., Nakanomyo, I., Ogawa, M., Sawa, S., Ohashi-Ito, K., Matsubayashi, Y. and Fukuda, H. (2008). Non-cell-autonomous control of vascular stem cell fate by a CLE peptide/receptor system. *Proc. Natl. Acad. Sci.* 105, 15208–15213.

Hirakawa, Y., Kondo, Y. and Fukuda, H. (2010). TDIF Peptide Signaling Regulates Vascular Stem Cell Proliferation via the *WOX4* Homeobox Gene in *Arabidopsis*. *Plant Cell* 22, 2618–2629.

Hu, J., Hu, X., Yang, Y., He, C., Hu, J. and Wang, X. (2022). Strigolactone signaling regulates cambial activity through repression of *WOX4* by transcription factor BES1. *Plant Physiol.* 188, 255–267.

Ikematsu, S., Tasaka, M., Torii, K. U. and Uchida, N. (2017). *ERECTA* -family receptor kinase genes redundantly prevent premature progression of secondary growth in the *Arabidopsis* hypocotyl. *New Phytol.* 213, 1697–1709.

Ito, Y., Nakanomyo, I., Motose, H., Iwamoto, K., Sawa, S., Dohmae, N. and Fukuda, H. (2006). Dodeca-CLE Peptides as Suppressors of Plant Stem Cell Differentiation. *Science* 313, 842–845.

Kiss, E., Oláh, B., Kaló, P., Morales, M., Heckmann, A. B., Borbola, A., Lózsa, A., Kontár, K., Middleton, P., Downie, J. A., et al. (2009). LIN, a Novel Type of U-Box/WD40 Protein, Controls Early Infection by Rhizobia in Legumes. *Plant Physiol.* 151, 1239–1249.

Kondo, Y., Ito, T., Nakagami, H., Hirakawa, Y., Saito, M., Tamaki, T., Shirasu, K. and Fukuda, H. (2014). Plant GSK3 proteins regulate xylem cell differentiation downstream of TDIF–TDR signalling. *Nat. Commun.* 5, 3504.

Kuppusamy, K. T., Endre, G., Prabhu, R., Penmetsa, R. V., Veereshlingam, H., Cook, D. R., Dickstein, R. and VandenBosch, K. A. (2004). *LIN* , a *Medicago truncatula* Gene Required for Nodule Differentiation and Persistence of Rhizobial Infections. *Plant Physiol.* 136, 3682–3691.

Lee, J. S., Kuroha, T., Hnilova, M., Khatayevich, D., Kanaoka, M. M., McAbee, J. M., Sarikaya, M., Tamerler, C. and Torii, K. U. (2012). Direct interaction of ligand–receptor pairs specifying stomatal patterning. *Genes Dev.* 26, 126–136.

Lenhard, M. and Laux, T. (2003). Stem cell homeostasis in the *Arabidopsis* shoot meristem is regulated by intercellular movement of CLAVATA3 and its sequestration by CLAVATA1. *Development* 130, 3163–3173.

Liu, H. and Stone, S. L. (2010). Abscisic Acid Increases *Arabidopsis* ABI5 Transcription Factor Levels by Promoting KEG E3 Ligase Self-Ubiquitination and Proteasomal Degradation. *Plant Cell* 22, 2630–2641.

Liu, H. and Stone, S. L. (2013). Cytoplasmic Degradation of the Arabidopsis Transcription Factor ABSCISIC ACID INSENSITIVE 5 Is Mediated by the RING-type E3 Ligase KEEP ON GOING. *J. Biol. Chem.* 288, 20267–20279.

Liu, C.-W., Breakspear, A., Stacey, N., Findlay, K., Nakashima, J., Ramakrishnan, K., Liu, M., Xie, F., Endre, G., De Carvalho-Niebel, F., et al. (2019). A protein complex required for polar growth of rhizobial infection threads. *Nat. Commun.* 10, 2848.

Liu, M., Jia, N., Li, X., Liu, R., Xie, Q., Murray, J. D., Downie, J. A. and Xie, F. (2021). CERBERUS is critical for stabilization of VAPYRIN during rhizobial infection in *Lotus japonicus*. *New Phytol.* 229, 1684–1700.

Lynch, T., Née, G., Chu, A., Krüger, T., Finkemeier, I. and Finkelstein, R. R. (2022). ABI5 binding protein2 inhibits ABA responses during germination without ABA-INSENSITIVE5 degradation. *Plant Physiol.* 189, 666–678.

Lyu, M., Iida, H., Eekhout, T., Mäkelä, M., Muranen, S., Ye, L., Vatén, A., Wybouw, B., Wang, X., De Rybel, B., et al. (2025). The dynamic and diverse nature of parenchyma cells in the Arabidopsis root during secondary growth. *Nat. Plants* 11, 878–890.

Mayer, K. F. X., Schoof, H., Haecker, A., Lenhard, M., Jürgens, G. and Laux, T. (1998). Role of WUSCHEL in Regulating Stem Cell Fate in the Arabidopsis Shoot Meristem. *Cell* 95, 805–815.

Mi, H., Lazareva-Ulitsky, B., Loo, R., Kejariwal, A., Vandergriff, J., Rabkin, S., Guo, N., Muruganujan, A., Doremieux, O., Campbell, M., et al. (2004). The PANTHER database of protein families, subfamilies, functions and pathways. *Nucleic Acids Res.* 33, D284–D288.

Mishra, A. K., Puranik, S. and Prasad, M. (2012). Structure and regulatory networks of WD40 protein in plants. *J. Plant Biochem. Biotechnol.* 21, 32–39.

Miyashima, S., Sebastian, J., Lee, J.-Y. and Helariutta, Y. (2012). Stem cell function during plant vascular development. *EMBO J.* 32, 178–193.

Ohashi-Ito, K., Kubo, M., Demura, T. and Fukuda, H. (2005). Class III Homeodomain Leucine-Zipper Proteins Regulate Xylem Cell Differentiation. *Plant Cell Physiol.* 46, 1646–1656.

Pan, X., Welti, R. and Wang, X. (2010). Quantitative analysis of major plant hormones in

crude plant extracts by high-performance liquid chromatography–mass spectrometry. *Nat. Protoc*. 5, 986–992.

Pauwels, L., Ritter, A., Goossens, J., Durand, A. N., Liu, H., Gu, Y., Geerinck, J., Boter, M., Vanden Bossche, R., De Clercq, R., et al. (2015). The RING E3 Ligase KEEP ON GOING Modulates JASMONATE ZIM-DOMAIN12 Stability. *Plant Physiol.* 169, 1405–1417.

Ragni, L. and Hardtke, C. S. (2014). Small but thick enough – the Arabidopsis hypocotyl as a model to study secondary growth. *Physiol. Plant.* 151, 164–171.

Ragni, L., Nieminen, K., Pacheco-Villalobos, D., Sibout, R., Schwechheimer, C. and Hardtke, C. S. (2011). Mobile Gibberellin Directly Stimulates *Arabidopsis* Hypocotyl Xylem Expansion. *Plant Cell* 23, 1322–1336.

Ramachandran, P., Wang, G., Augstein, F., De Vries, J. and Carlsbecker, A. (2018). Continuous root xylem formation and vascular acclimation to water deficit involves endodermal ABA signalling via miR165. *Development* dev.159202.

Sayers, E. W., Beck, J., Bolton, E. E., Brister, J. R., Chan, J., Connor, R., Feldgarden, M., Fine, A. M., Funk, K., Hoffman, J., et al. (2025). Database resources of the National Center for Biotechnology Information in 2025. *Nucleic Acids Res.* 53, D20–D29.

Schaller, G. E., Bishopp, A. and Kieber, J. J. (2015). The Yin-Yang of Hormones: Cytokinin and Auxin Interactions in Plant Development. *Plant Cell* 27, 44–63.

Schoof, H., Lenhard, M., Haecker, A., Mayer, K. F. X., Jürgens, G. and Laux, T. (2000). The Stem Cell Population of Arabidopsis Shoot Meristems Is Maintained by a Regulatory Loop between the CLAVATA and WUSCHEL Genes. *Cell* 100, 635–644.

Serra, O., Mähönen, A. P., Hetherington, A. J. and Ragni, L. (2022). The Making of Plant Armor: The Periderm. *Annu. Rev. Plant Biol.* 73, 405–432.

Shpak, E. D., Lakeman, M. B. and Torii, K. U. (2003). Dominant-Negative Receptor Uncovers Redundancy in the Arabidopsis ERECTA Leucine-Rich Repeat Receptor–Like Kinase Signaling Pathway That Regulates Organ Shape. *Plant Cell* 15, 1095–1110.

Shpak, E. D., Berthiaume, C. T., Hill, E. J. and Torii, K. U. (2004). Synergistic interaction of three ERECTA-family receptor-like kinases controls *Arabidopsis* organ growth and flower development by promoting cell proliferation. *Development* 131, 1491–1501.

Shpak, E. D., McAbee, J. M., Pillitteri, L. J. and Torii, K. U. (2005). Stomatal Patterning and Differentiation by Synergistic Interactions of Receptor Kinases. *Science* 309, 290–293.

Sibout, R., Plantegenet, S. and Hardtke, C. S. (2008). Flowering as a Condition for Xylem Expansion in Arabidopsis Hypocotyl and Root. *Curr. Biol.* 18, 458–463.

Smetana, O., Mäkilä, R., Lyu, M., Amiryousefi, A., Sánchez Rodríguez, F., Wu, M.-F., Solé-Gil, A., Leal Gavarrón, M., Siligato, R., Miyashima, S., et al. (2019). High levels of auxin signalling define the stem-cell organizer of the vascular cambium. *Nature* 565, 485–489.

Smit, M. E., McGregor, S. R., Sun, H., Gough, C., Bågman, A.-M., Soyars, C. L., Kroon, J. T., Gaudinier, A., Williams, C. J., Yang, X., et al. (2020). A PXY-Mediated Transcriptional Network Integrates Signaling Mechanisms to Control Vascular Development in Arabidopsis. *Plant Cell* 32, 319–335.

Stephenson, N. L., Das, A. J., Condit, R., Russo, S. E., Baker, P. J., Beckman, N. G., Coomes, D. A., Lines, E. R., Morris, W. K., Rüger, N., et al. (2014). Rate of tree carbon accumulation increases continuously with tree size. *Nature* 507, 90–93.

Stone, S. L., Williams, L. A., Farmer, L. M., Vierstra, R. D. and Callis, J. (2007). KEEP ON GOING, a RING E3 Ligase Essential for *Arabidopsis* Growth and Development, Is Involved in Abscisic Acid Signaling. *Plant Cell* 18, 3415–3428.

Suer, S., Agusti, J., Sanchez, P., Schwarz, M. and Greb, T. (2011). *WOX4* Imparts Auxin Responsiveness to Cambium Cells in *Arabidopsis*. *Plant Cell* 23, 3247–3259.

Sundell, D., Street, N. R., Kumar, M., Mellerowicz, E. J., Kucukoglu, M., Johnsson, C., Kumar, V., Mannapperuma, C., Delhomme, N., Nilsson, O., et al. (2017). AspWood: High-Spatial-Resolution Transcriptome Profiles Reveal Uncharacterized Modularity of Wood Formation in *Populus tremula*. *Plant Cell* 29, 1585–1604.

Tajdel-Zielińska, M., Janicki, M., Marczak, M. and Ludwików, A. (2024). *Arabidopsis* HECT and RING-type E3 Ligases Promote MAPKKK18 Degradation to Regulate Abscisic Acid Signaling. *Plant Cell Physiol.* 65, 390–404.

Takata, N., Yokota, K., Ohki, S., Mori, M., Taniguchi, T. and Kurita, M. (2013). Evolutionary Relationship and Structural Characterization of the EPF/EPFL Gene Family. *PLoS ONE* 8, e65183.

Teyssendier De La Serve, J., Gautrat, P., Laffont, C., Lesterps, Z., Huault, E., Guerard, F., San Clemente, H., Aguilar, M., Bensmihen, S., Gakière, B., et al. (2025). The sTDIF signaling peptide modulates the root stele diameter and primary metabolism to accommodate symbiotic nodulation. *Curr. Biol.* 35, 4337-4348.e4.

Tisné, S., Barbier, F. and Granier, C. (2011). The ERECTA gene controls spatial and temporal patterns of epidermal cell number and size in successive developing leaves of Arabidopsis thaliana. *Ann. Bot.* 108, 159–168.

Torii, K. U., Mitsukawa, N., Oosumi, T., Matsuura, Y., Yokoyama, R., Whittier, R. F. and Komeda, Y. (1996). The Arabidopsis ERECTA gene encodes a putative receptor protein kinase with extracellular leucine-rich repeats. *Plant Cell* 8, 735–746.

Turley, E. K. and Etchells, J. P. (2022). Laying it on thick: a study in secondary growth. *J. Exp. Bot.* 73, 665–679.

Uchida, N. and Tasaka, M. (2013). Regulation of plant vascular stem cells by endodermis-derived EPFL-family peptide hormones and phloem-expressed ERECTA-family receptor kinases. *J. Exp. Bot.* 64, 5335–5343.

Uchida, N. and Torii, K. U. (2019). Stem cells within the shoot apical meristem: identity, arrangement and communication. *Cell. Mol. Life Sci.* 76, 1067–1080.

Uchida, N., Lee, J. S., Horst, R. J., Lai, H.-H., Kajita, R., Kakimoto, T., Tasaka, M. and Torii, K. U. (2012). Regulation of inflorescence architecture by intertissue layer ligand–receptor communication between endodermis and phloem. *Proc. Natl. Acad. Sci.* 109, 6337–6342.

Wang, N., Bagdassarian, K. S., Doherty, R. E., Kroon, J. T., Connor, K. A., Wang, X. Y., Wang, W., Jermyn, I. H., Turner, S. R. and Etchells, J. P. (2019). Organ-specific genetic interactions between paralogues of the *PXY* and *ER* receptor kinases enforce radial patterning in *Arabidopsis* vascular tissue. *Development* dev.177105.

Wu, S. and Gallagher, K. L. (2014). The movement of the non-cell-autonomous transcription factor, SHORT-ROOT relies on the endomembrane system. *Plant J.* 80, 396–409.

Xiao, T. T., Schilderink, S., Moling, S., Deinum, E. E., Kondorosi, E., Franssen, H., Kulikova, O., Niebel, A. and Bisseling, T. (2014). Fate map of *Medicago truncatula* root nodules. *Development* 141, 3517–3528.

Yadav, R. K., Perales, M., Gruel, J., Ohno, C., Heisler, M., Girke, T., Jönsson, H. and Reddy, G. V. (2013). Plant stem cell maintenance involves direct transcriptional repression of differentiation program. *Mol. Syst. Biol.* 9,.

Yadav, V., Arif, N., Singh, V. P., Guerriero, G., Berni, R., Shinde, S., Raturi, G., Deshmukh, R., Sandalio, L. M., Chauhan, D. K., et al. (2021). Histochemical Techniques in Plant Science: More Than Meets the Eye. *Plant Cell Physiol.* 62, 1509–1527.

Yang, J. H., Lee, K., Du, Q., Yang, S., Yuan, B., Qi, L. and Wang, H. (2020a). A membrane-associated NAC domain transcription factor XVP interacts with TDIF co-receptor and regulates vascular meristem activity. *New Phytol.* 226, 59–74.

Yang, S., Wang, S., Li, S., Du, Q., Qi, L., Wang, W., Chen, J. and Wang, H. (2020b). Activation of ACS7 in Arabidopsis affects vascular development and demonstrates a link between ethylene synthesis and cambial activity. *J. Exp. Bot.* 71, 7160–7170.

Ye, L., Wang, X., Lyu, M., Siligato, R., Eswaran, G., Vainio, L., Blomster, T., Zhang, J. and Mähönen, A. P. (2021). Cytokinins initiate secondary growth in the Arabidopsis root through a set of LBD genes. *Curr. Biol.* 31, 3365-3373.e7.

Zhang, H., Lin, X., Han, Z., Wang, J., Qu, L.-J. and Chai, J. (2016). SERK Family Receptor-like Kinases Function as Co-receptors with PXY for Plant Vascular Development. *Mol. Plant* 9, 1406–1414.

Zhou, G.-K., Kubo, M., Zhong, R., Demura, T. and Ye, Z.-H. (2007). Overexpression of miR165 Affects Apical Meristem Formation, Organ Polarity Establishment and Vascular Development in Arabidopsis. *Plant Cell Physiol.* 48, 391–404.

## 6.0 Appendices

6.1 Expression patterns of Poplar genes homologous to *Arabidopsis PUCK*.

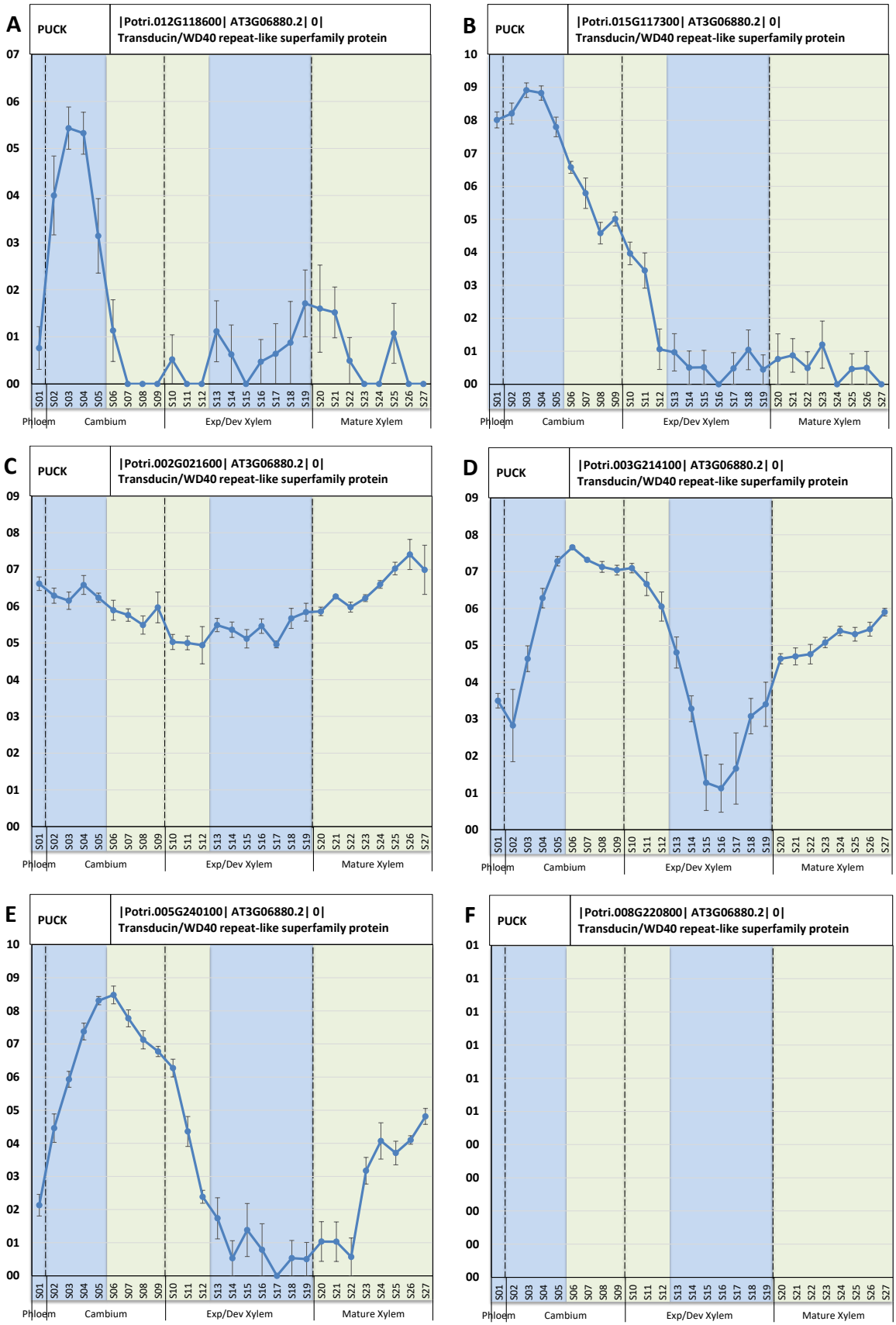

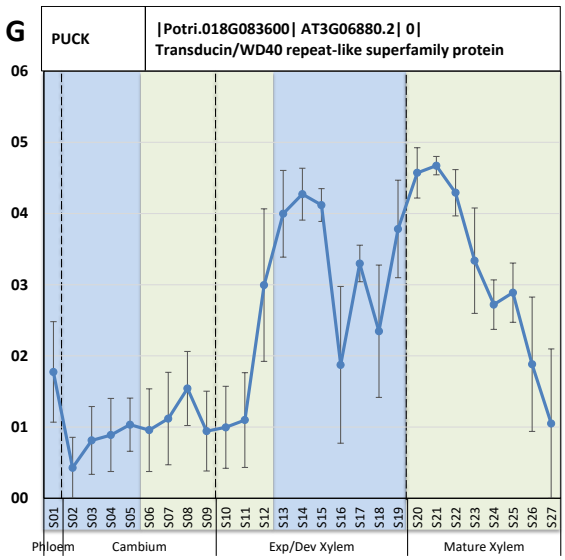


Supplementary Figure 1, Expression patterns of Poplar homologues to PUCK. Poplar has 7 PUCK homologues, A-G (Sundell et al., 2017).

## 6.2 Results of statistical tests for histochemical stained *puck* mutant images

Supplementary Table 1, The results of statistical tests on the radius of the xylem, performed in R.

| Test | Test Statistic | p Value | Meaning |
|---|---|---|---|
| Shapiro-Wilk Normality Test | W = 0.968 | p = 0.0761 | p > 0.05, not significant, data is normally distributed |
| Levene's Test for Homogeneity of Variances | F = 1.32 | p = 0.274 | p > 0.05, not significant, variances are equal |
| One-way ANOVA | F = 7.89 | p = 0.000135 | p < 0.05, significant, difference in xylem radius between genotypes |
| Tukey Multiple Comparison of Means | n/a | WT - *puck* = 0.375<br>WT - *pxy* = 0.0992<br>WT - *pxy puck* = 0.0000519<br>*puck* - *pxy* = 0.913<br>*puck* - *pxy puck* = 0.0141<br>*pxy* - *pxy puck* = 0.0608 | Significant differences WT - *pxy puck,* and *puck* - *pxy puck* |

Supplementary Table 2, The results of statistical tests on the number of lignified cells in a 90° segment of the xylem, performed in R.

| Test | Test Statistic | p Value | Meaning |
|---|---|---|---|
| Shapiro-Wilk Normality Test | W = 0.937 | p = 0.000193 | p < 0.05, significant, data is not normally distributed |
| Levene's Test for Homogeneity of Variances | F = 1.81 | p = 0.154 | p > 0.05, not significant, variances are equal |
| Kruskal-Wallis Rank Sum Test | Chi-squared = 10.1 | p = 0.0178 | p < 0.05, significant, difference in lignified cells between genotypes |
| Wilcoxon Rank Sum Test with Continuity Correction | n/a | WT - *puck* = 1.00<br>WT - *pxy* = 0.152<br>WT - *pxy puck* = 1.00<br>*puck* - *pxy* = 0.0160<br>*puck* - *pxy puck* = 1.00<br>*pxy* - *pxy puck* = 0.113 | Significant differences *puck* - *pxy* only |

Supplementary Table 3, The results of statistical tests on the number of neighbours the central xylem cell has, performed in R. Data is ordinal so Kruskal-Wallis must be used.

| Test | Test Statistic | p Value | Meaning |
|---|---|---|---|
| Kruskal-Wallis Rank Sum Test | Chi-squared = 12.2 | p = 0.00661 | p < 0.05, significant, difference in neighbours between genotypes |
| Wilcoxon Rank Sum Test with Continuity Correction | n/a | WT - *puck* = 0.0850<br>WT - *pxy* = 0.647<br>WT - *pxy puck* = 0.647<br>*puck* - *pxy* = 0.0220<br>*puck* - *pxy puck* = 0.0240<br>*pxy* - *pxy puck* = 0.654 | Significant differences *puck* - *pxy* and *puck* - *pxy puck* |

Supplementary Table 4, The results of statistical tests on phloem width, performed in R.

| Test | Test Statistic | p Value | Meaning |
|---|---|---|---|
| Shapiro-Wilk Normality Test | W = 0.943 | p = 0.00363 | p < 0.05, significant, data is not normally distributed |
| Levene's Test for Homogeneity of Variances | F = 6.60 | p = 0.000589 | p < 0.05, significant, variances are not equal |
| Kruskal-Wallis Rank Sum Test | Chi-squared = 44.7 | p = 1.08e-09 | p < 0.05, significant, difference in phloem width between genotypes |
| Wilcoxon Rank Sum Test with Continuity Correction | n/a | WT - *puck* = 0.315<br>WT - *pxy* = 1.70e-06<br>WT - *pxy puck* = 1.30e-05<br>*puck* - *pxy* = 3.10e-05<br>*puck* - *pxy puck* = 0.00280<br>*pxy* - *pxy puck* = 0.00360 | Significant differences *WT - pxy, WT - pxy puck, puck - pxy, puck - pxy puck* and *pxy - pxy puck* |

Supplementary Table 5, The results of statistical tests on the intercalation of phloem within the xylem tissue, performed in R. Data is ordinal so Kruskal-Wallis must be used.

| Test | Test Statistic | p Value | Meaning |
|---|---|---|---|
| Kruskal-Wallis Rank Sum Test | Chi-squared = 39.3 | p = 1.51e-08 | p < 0.05, significant, difference in intercalation between genotypes |
| Wilcoxon Rank Sum Test with Continuity Correction | n/a | WT - *puck* = 0.462<br>WT - *pxy* = 2.90e-05<br>WT - *pxy puck* = 1.10e-06<br>*puck* - *pxy* = 0.00329<br>*puck* - *pxy puck* = 0.000240<br>*pxy* - *pxy puck* = 0.231 | Significant differences WT - *pxy,* WT - *pxy puck, puck - pxy,* and *puck - pxy puck* |